


## REVIEW

[View Article Online](#)  
[View Journal](#) | [View Issue](#)Cite this: *J. Mater. Chem. A*, 2023, **11**, 6796Received 29th November 2022  
Accepted 19th February 2023

DOI: 10.1039/d2ta09286g

[rsc.li/materials-a](https://rsc.li/materials-a)

## Various approaches to synthesize water-stable halide PeNCs

Avijit Das,<sup>†</sup> Arup Ghorai,<sup>†</sup> Kundan Saha, Arka Chatterjee and Unyong Jeong <sup>\*</sup>

The “halide perovskite fever” is ongoing in material-based research due to the extraordinary properties of halide perovskites like high absorption coefficient, tunable band gap (throughout the visible range), near-unity emission quantum yield, large carrier diffusion length (exceeding 1  $\mu\text{m}$ ), and a long recombination time ( $\sim\mu\text{s}$  order). However, the water instability of halide perovskites is an Achilles’ heel that must be overcome. Recently, some approaches have been adopted to improve the water stability of  $\text{ABX}_3$  perovskites, including the substitution of A cations, ligand exchange, encapsulation in porous frameworks, passivation with inorganic or organic layers, and encapsulation in hydrophobic polymers and glass matrices. This review briefly introduces the degradation mechanisms according to the RH and summarizes various approaches to stabilize halide perovskites. An outlook for research directions of halide perovskites is also suggested.

## 1. Introduction

Solution-processed halide PeNCs have already set benchmarks in the research on optical devices<sup>1–4</sup> and optoelectronic devices,<sup>5–7</sup> especially solar cells<sup>8–11</sup> (making them competitors to Si-based solar cells in terms of efficiency) and solid-state light-emitting diodes (providing outstanding colour purity and high luminescence efficiency).<sup>12–17</sup> Despite the relatively short period of research, perovskite nanocrystals (PeNCs) achieved almost  $\sim 30\%$  power conversion efficiency (PCE),<sup>10</sup> near-unity photoluminescence quantum yield (PLQY),<sup>14,18</sup> large carrier lifetime ( $\geq 1 \mu\text{s}$ ),<sup>19</sup> and long carrier diffusion length (in the range of  $\mu\text{m}$ ).<sup>20</sup> However, instability in the presence of water impedes large-scale commercialization or daily use of products. Conventional emitters like inorganic chalcogenide nanocrystals and organic emitters exceed  $10^6$  hours of lifetime ( $\text{LT}_{50}$  = initial luminance dropping to 50% of the original value) with very low thermal stability.<sup>21</sup> The PeNCs should meet the air/water stability criterion for commercialization, which is over 10 000 hours of lifetime at about  $5000 \text{ cd m}^{-2}$  needed for outdoor display applications.<sup>22</sup> The instability is attributed largely to their low formation energy (0.1–0.6 eV) and the intrinsic ionic nature,<sup>23,24</sup> making the PeNCs unstable in various external stimuli (water, light, and electric field).<sup>25,26</sup> Another big concern in the case of lead halide perovskites is toxicity.<sup>27</sup> These obstacles have brought extensive research on underwater stabilization of PeNCs and the reduction of toxicity, especially by

encapsulating or replacing toxic Pb with Sn, Ag or Bi for industrial standards.

A variety of synthetic strategies have been explored to stabilize PeNCs under ambient conditions. Initially, the replacement of organic cations by inorganic cations like  $\text{Cs}^+$ ,  $\text{Rb}^+$ , and  $\text{Bi}^{3+}$  was found to improve the thermal and water stabilities by many times even though it was not enough for commercialization.<sup>28,29</sup> The hybrid perovskites may immediately degrade to their non-perovskite phase even under low humidity conditions because water molecules can form hydrogen bonding with the organic cations.<sup>26,30</sup> Another important parameter to determine the stability of perovskites is the Goldschmidt tolerance factor ( $\tau$ ). It can be defined by  $\tau = \frac{r_A + r_B}{\sqrt{2}(r_B + r_X)}$ , where  $r_A$ ,  $r_B$ , and  $r_X$  are the effective ionic radii of the A, B, and X site atoms of the general form of the  $\text{ABX}_3$  perovskite. In a simple way, it indicates how the A cation can be fitted within the structural cage.<sup>31</sup> Stability increases as the  $\tau$  value approaches unity. Especially, since iodine-based perovskites have low  $\tau$  values in the range of  $\sim 0.85$ – $0.9$ , they are prone to degradation compared to the bromide- or chloride-based perovskites ( $\tau \geq 0.9$ ). It is often reported that inorganic perovskites can transform to 0D ( $\text{Cs}_4\text{PbI}_6$ ), 3D ( $\text{CsPbI}_3$ ), and 2D ( $\text{CsPb}_2\text{X}_5$ ) crystals at low relative humidity (RH) without much degradation in their optical properties;<sup>26</sup> however, they degrade to the non-perovskite  $\delta$ -phase in an aqueous solution (excess water). Now that commercial products are required to be stable in the water medium, this approach needs to be modified. Research has evolved to bi- or tri-cation substitutions to further enhance the stability under humid conditions.<sup>32,33</sup> Also, the 2D/3D hybrid perovskite strategies are often used to utilize both exceptional optical properties of 3D perovskites and water immunity by 2D perovskites.<sup>34,35</sup> Recently,

Department of Materials Science and Engineering, Pohang University of Science and Technology, 77 Cheongam-Ro, Nam-Gu, Pohang 37673, Republic of Korea. E-mail: [u jeong@postech.ac.kr](mailto:u jeong@postech.ac.kr)

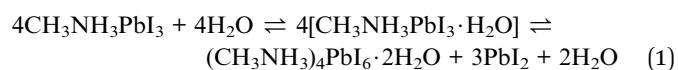
<sup>†</sup> They contributed equally.

new approaches have been explored. Surface passivation with a hydrophobic layer,<sup>36</sup> porous materials,<sup>37,38</sup> polymers,<sup>39</sup> or inorganic materials has improved the stability of PeNCs under robust ambient conditions. Polymer coating of the PeNC surface and embedding PeNCs in a polymer matrix or glass matrix are good ways in terms of protecting water penetration as well as retention of PLQY.<sup>40–42</sup>

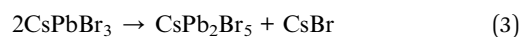
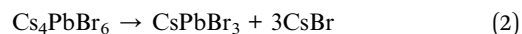
In this review, we provide a summary of recent advances in water stability, with a particular emphasis on the passivation and embedding of PeNCs or films as novel stabilization approaches. Section 2 briefly summarizes the degradation mechanism of PeNCs in the presence of water. Section 3 discusses conventional stabilization strategies such as cation substitution and ligand exchange. Section 4 introduces relatively new passivation strategies including insertion of PeNCs in a porous medium, encapsulation with inorganic nanomaterials, surface passivation with a hydrophobic/hydrophilic organic layer, and *in situ* growth in a polymer/glass matrix. This article ends with an outlook for future research directions.

## 2. Degradation by water: hydration, transformation, decomposition, and dissolution

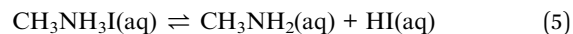
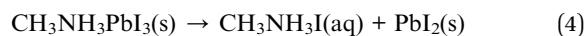
The structure, composition, and optical characteristics of PeNCs are significantly affected by water molecules. The type of interaction with water molecules is dependent on the molar ratio of water to NCs. Formamidinium lead halide (FAPbX<sub>3</sub>), methyl ammonium lead halide (MAPbX<sub>3</sub>), and lead-free hybrid perovskites are likely to be hydrated by water molecules under low RH conditions (Fig. 1A–C).<sup>30,43–45</sup> Water molecules can interact through hydrogen bonding with the uncoordinated ions and form mono-hydrated and di-hydrated structures (Fig. 1B). This hydration is a reversible process.<sup>46</sup> Mosconi *et al.* thoroughly investigated the interaction of water molecules and MAPbI<sub>3</sub>, and they presented a model in which water molecules can penetrate into the MAPbI<sub>3</sub> crystals to form hydrogen bonds with the methyl ammonium (MA) cations.<sup>47</sup> The formation of the intermediate hydrated phase was experimentally proved through time-resolved photoluminescence (PL) measurements and infrared (IR) spectroscopy.<sup>47,48</sup> Christians *et al.* reported that water molecules are also able to form a di-hydrated complex with the MAPbI<sub>3</sub> even under dark conditions.<sup>49</sup> The hydration leads to significant changes in the crystal structure, thereby in optical and electronic properties.<sup>50</sup> Yang *et al.*<sup>51</sup> systematically investigated the perovskite degradation process under controlled RH conditions by using *in situ* absorption spectroscopy and *in situ* grazing incidence X-ray diffraction. These studies confirmed the formation of hydrated products in the initial degradation step. The sequential perovskite hydration can be described using eqn (1):



Unlike hybrid perovskites, all-inorganic perovskites undergo phase transformation under a low relative humidity atmosphere (Fig. 1C). For instance, Turedi *et al.* found that the interaction between water and three-dimensional (3D) perovskite CsPbBr<sub>3</sub> can induce the phase transformation to two-dimensional (2D) perovskite-related CsPb<sub>2</sub>Br<sub>5</sub> where the coordination number of Pb(II) changes from six to eight.<sup>52</sup> Similarly, Lin *et al.* reported that a stable hydration shell can be formed on the surface of the Cs<sub>4</sub>PbBr<sub>6</sub> (0D) crystals in the presence of water and the Cs<sub>4</sub>PbBr<sub>6</sub> transforms into 3D corner-sharing CsPbBr<sub>3</sub>, and then into 2D edge-sharing CsPb<sub>2</sub>Br<sub>5</sub>,<sup>53</sup> which can be illustrated using eqn (2) and (3).<sup>54</sup>



Yu *et al.* reported reversible restoration of the luminescent CsPbBr<sub>3</sub> phase from the non-luminescent CsPb<sub>2</sub>Br<sub>5</sub> phase upon the removal of water.<sup>55</sup> In contrast to the reversible hydration and phase transformation taking place at low RH, irreversible degradation occurs when PeNCs are continuously exposed to a high RH atmosphere and hence PbX<sub>2</sub> and AX are formed spontaneously (Fig. 1D) which can be explained using eqn (4) and (5).<sup>46,56,57</sup>



Recently, Siegler *et al.* revealed that the degradation kinetics of MAPbI<sub>3</sub> NC also can take place through a water-accelerated photo-oxidation.<sup>58</sup> Moreover, the degradation process takes place more rapidly under UV irradiation and oxygen exposure because the CH<sub>3</sub>NH<sub>3</sub><sup>+</sup> bonding becomes weakened.<sup>59</sup> Ho *et al.* reported that FA<sub>0.85</sub>Cs<sub>0.15</sub>PbI<sub>3</sub> could be completely degraded to δo-CsPbI<sub>3</sub>, δ-FAPbI<sub>3</sub>, FA, and PbI<sub>2</sub> through a multistep pathway at a high RH.<sup>60</sup> In this case, the optical and electrical properties are mostly lost. For instance, Huang *et al.* reported a 90% loss of PL intensity in CsPbBr<sub>3</sub> under high RH conditions.<sup>61</sup> Christians *et al.* found a significant drop in photovoltaic efficiency of the CH<sub>3</sub>NH<sub>3</sub>PbI<sub>3</sub> perovskite from 12% to 1% after 3 days of exposure to 90% RH.<sup>49</sup> Caddeo *et al.* studied the degradation process by finite-temperature molecular dynamics and revealed that the decomposition kinetics is temperature dependent with an activation energy of 0.36 eV and the aggregated water molecules act as a catalyst to form the defects on PeNCs during the degradation process.<sup>62</sup> Wu *et al.* reported that Pb-containing PeNCs has a high solubility constant ( $K_{\text{sp}} = 10^{-8}$ ) in an aqueous solution.<sup>63</sup> Thus, the complete dissolution of perovskite crystals takes place in the aqueous precursor solution when the amount of water increases up to a threshold (Fig. 1E). For example, Hailegnaw *et al.* reported the complete decomposition of MAPbI<sub>3</sub>-based solar cells under exposure to rainwater where methylammonium lead iodide was decomposed to hydroiodic acid, methylamine, and lead iodide.<sup>64</sup> The original black/dark brown color turned yellow and the device performance was significantly reduced. Ionized ions of Pb<sup>2+</sup>, Cs<sup>+</sup>, and X<sup>−</sup> could be

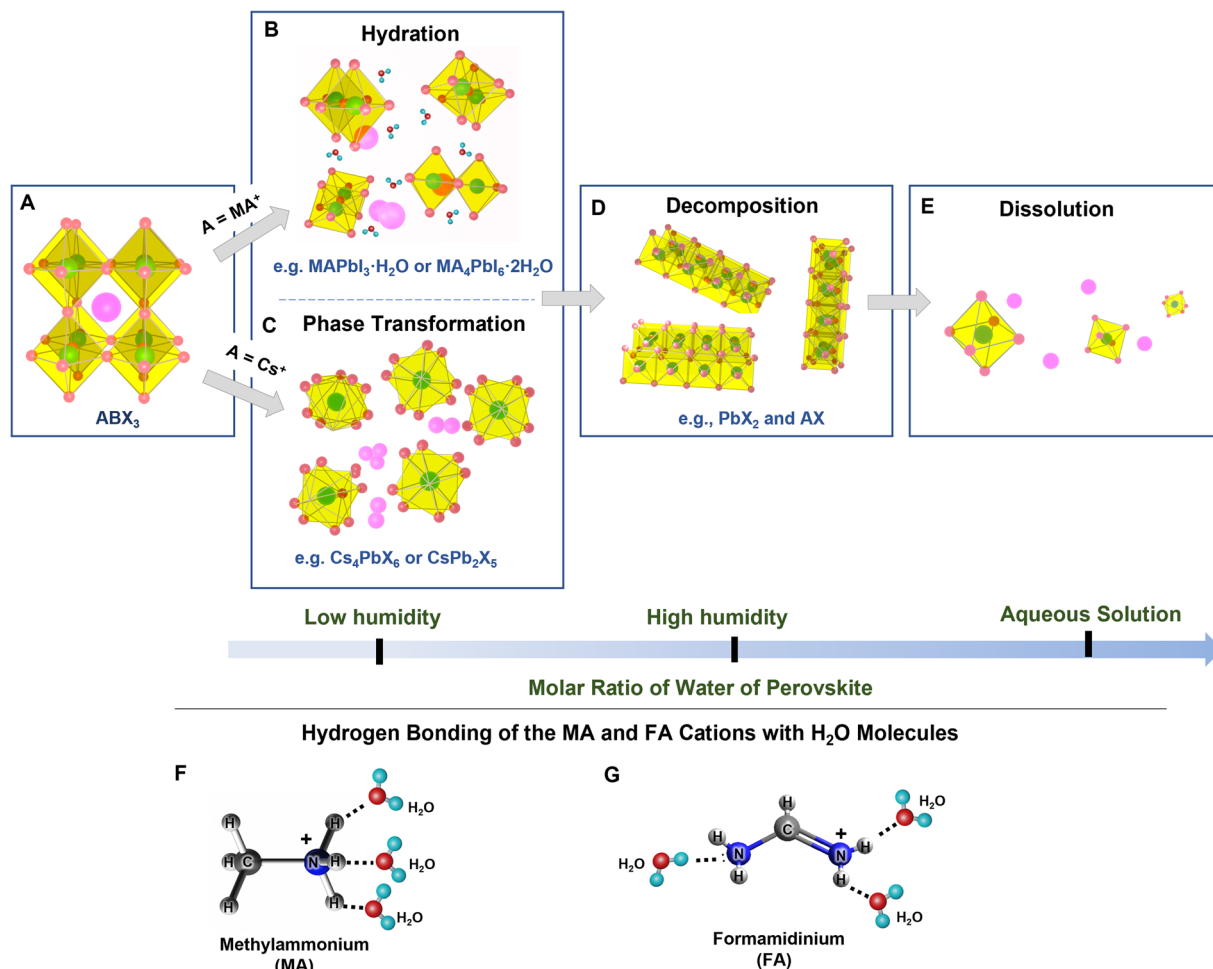
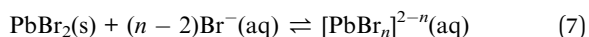
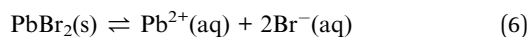


Fig. 1 (A–E) Schematic representations of the interactions between water molecules and halide PeNCs (modified with permission from ref. 26). (F and G) Schematic representations of the formation of the hydrogen bonding of methylammonium (F) and formamidineium (G) cations with water molecules.

formed in the presence of an excess amount of water (eqn (6)), but sometimes  $X^-$  can inhibit the ionization of  $PbX_2$  and form  $[PbX_n]^{2-n}$  as shown in eqn (7).<sup>65</sup>



Overall, a thorough knowledge of the interaction between water molecules and PeNCs is of significant importance in the development of water-stable perovskites and devices for real-life applications.<sup>66,67</sup>

### 3. Stabilization of PeNCs

#### 3.1. Substitution of A cations

The  $ABX_3$  formula is commonly used to describe halide perovskites, where the A-site is an inorganic cation (often  $Cs^+$ ,  $Rb^+$ , or  $K^+$ ) or an organic alkyl cation (typically,  $CH_3NH_3^+$  ( $MA^+$ ) or  $NH_2CHNH_2^+$  ( $FA^+$ )) (Fig. 2A), which fills the cuboctahedral voids. Trimethyl sulphonium ions are also used to synthesize

air-stable lead halide perovskites,<sup>68</sup> in order to counterbalance  $[BX_6]^{4-}$  and stabilize the perovskite lattice. The cations can be categorized as mono, double, triple, or quadruple A-cation perovskites according to the number of A-site cations present in the crystal lattice. The crystal structures can be varied especially depending on the Goldschmidt tolerance factor (GTF) which normally falls in the range of 0.8–1.0.<sup>32</sup> The GTF determines the ambient stability as well as the phase stability of PeNCs. When the GTF is close to 1, it leads to maximum ambient stability. In the case of organic–inorganic hybrid perovskites, the organic counterpart is responsible for the lower ambient stability due to its volatile nature. For example, the absorption intensity of  $MAPbI_3$  was considerably reduced at a high RH (98%) within 4 h with a blue-shifted absorption band edge, but the degradation took approximately 10 000 h at a lower RH (20%).<sup>69</sup> Even doping with inorganic chalcogenides like  $PbSe$  enhances the stability as well as device performance of  $MAPbX_3$ -based solar cells, with moisture stability enhanced 200 fold.<sup>70</sup>

**3.1.1. Inorganic cations.** It is well known that water molecules quickly transform the photoactive black phase of  $FAPbI_3$  into a photo-inactive yellow phase. The effective hydrogen

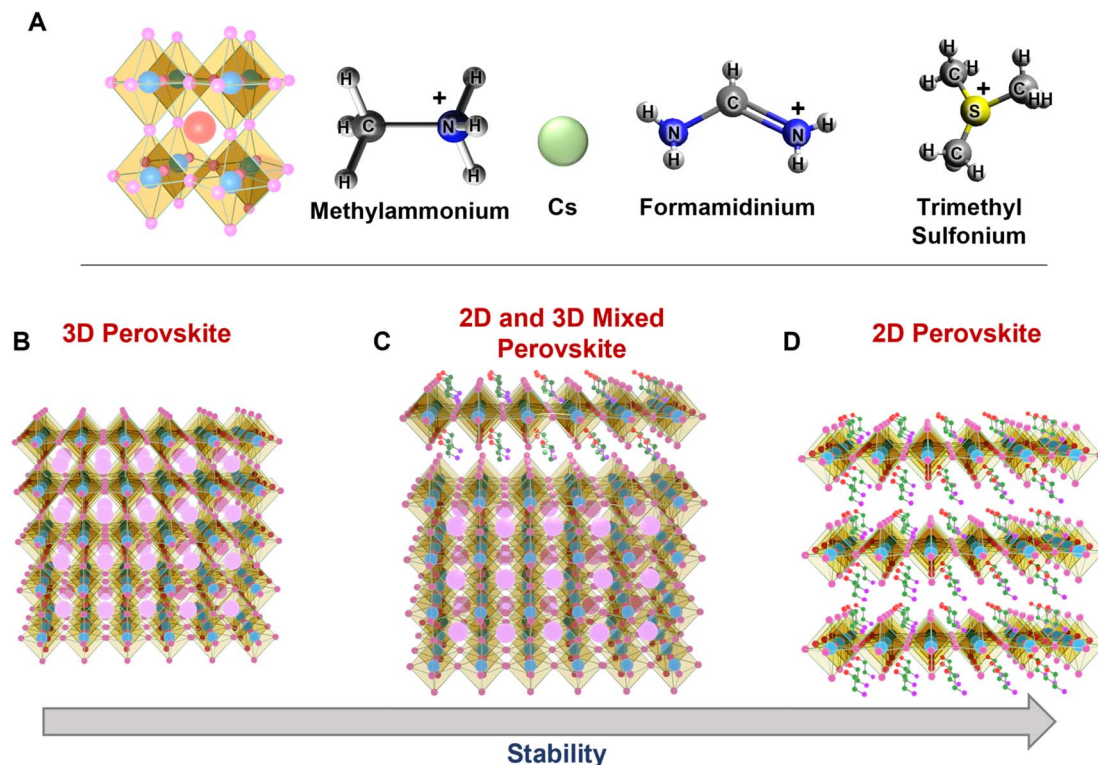


Fig. 2 (A) The perovskite unit cell consisting of an A cation (methylammonium, Cs, formamidinium, trimethyl sulfonium) at the center, (B–D) schematic illustration depicting the crystalline structure of 3D perovskites (B), mixed-dimensionality perovskites (C), and 2D perovskites (D).

bonding of the methylammonium cation (MA<sup>+</sup>) and formamidinium cation (FA<sup>+</sup>) with water molecules is responsible for the instability of MAPbI<sub>3</sub> and FAPbI<sub>3</sub>.<sup>71</sup> Also, weak electrostatic interaction between the MA<sup>+</sup> and [PbI<sub>6</sub>]<sup>4–</sup> is another potential reason for the prompt degradation.<sup>69</sup> In that sense, inorganic halide perovskites exhibit better thermal water stability than their hybrid family because of the absence of the bonding between Cs<sup>+</sup> with the water molecule.<sup>26</sup> Simply mixing the A-site cations with metals has been employed for improved water stability. Mixing a small fraction of stable Cs<sup>+</sup> with the FA or MA-based perovskite successfully suppressed the formation of the optically inactive  $\delta$ -phase by adjusting the GTF factor.<sup>72</sup> Park *et al.* demonstrated that when 10% of FA<sup>+</sup> was replaced by Cs<sup>+</sup> in FAPbI<sub>3</sub> the water stability was improved and photo-degradation under constant UV illumination was minimized.<sup>73</sup> Under continuous UV illumination (intensity =  $\sim 100$  mW cm<sup>–2</sup>) for 19 h, the FAPbI<sub>3</sub> film showed 86% degradation, but the FA<sub>0.9</sub>Cs<sub>0.1</sub>PbI<sub>3</sub> film showed 65% degradation. Under 85% humidity conditions for 7 h, the FAPbI<sub>3</sub> film had 77.8% degradation; meanwhile, the FA<sub>0.9</sub>Cs<sub>0.1</sub>PbI<sub>3</sub> film showed 50% degradation. Wu *et al.* further observed that using triple cation Cs/MA/FA was more robust in terms of stability, reproducibility, and efficiency. They have reported that perovskite NCs showed long-term stability for up to one month under 30% RH and PCE above 20%.<sup>74</sup>

**3.1.2. Organic cations.** 2D perovskites have recently drawn immense attention due to their superior stability and water resistance compared to 3D perovskites. 2D layered perovskites

are represented as R<sub>2</sub>(CH<sub>3</sub>NH<sub>3</sub>)<sub>n–1</sub>B<sub>n</sub>X<sub>3n+1</sub>, where *n*, R, B, and X denote the number of inorganic layers, organic cations such as C<sub>6</sub>H<sub>5</sub>(CH<sub>2</sub>)<sub>2</sub>NH<sub>3</sub><sup>+</sup> (phenyl-ethyl ammonium, PEA), a metal cation, and a halide, respectively. The improved moisture resistance of 2D perovskites comes from the presence of the hydrophobic R group shown in Fig. 2B. The R-groups occupy the surface site of the crystals and protect them from water penetration. Sargent and colleagues generated a series of dimension-controlled quasi-2D MAPbBr<sub>3</sub> perovskites *via* partial substitution of MAs by hydrophobic phenethylamine (PEA) molecules.<sup>75</sup> The moisture stability was improved after this process. The PEA-substituted MAPbI<sub>3</sub> film showed a negligible change in the adsorption edge and PL intensity after storage under 90% humidity conditions for 3 months. Romani *et al.* recently synthesized a 2D lead-free metal halide perovskite (PEA<sub>2</sub>SnBr<sub>4</sub>) showing impressive and unprecedented water resistance in both structural and optical properties.<sup>76</sup> PEA<sub>2</sub>SnBr<sub>4</sub> did not alter its Sn<sup>2+</sup> oxidation peak position (487.6 eV) in XPS even after continuous stirring in water for 4 h. It is notable that partial substitution of the anions by SCN functional groups also improved the moisture stability.<sup>77</sup> The SCN-substituted film exhibited prolonged stability for 4 h under 95% high humid conditions compared to the normal CH<sub>3</sub>NH<sub>3</sub>PbI<sub>3</sub> film (2.5 h). One of the concerns regarding organic molecular capping is that the dielectric organic layer hinders efficient carrier insertion and anisotropic charge transport. Coating a 2D layer on top of the 3D perovskite (2D/3D hybrid) has been investigated as a promising approach to simultaneously obtain water stability



and good charge transport. Liu *et al.* achieved extraordinary long-term stability (>10 000 h, or >400 days) with no reduction in efficiency over a vast area by depositing pentafluorophenyl ethylammonium (FEA) lead iodide  $[(\text{FEA})_2\text{PbI}_4]$ , which is a superhydrophobic 2D perovskite, onto the 3D  $\text{FAPbI}_3$  perovskite films.<sup>78</sup> The highly stable perovskites allowed the fabrication of a fully printable, low-cost, high-efficiency solar module that can be assessed under standard settings and in the presence of oxygen and moisture.<sup>79</sup>

### 3.2. Ligand exchange

Ligands in perovskites play a vital role in stability and morphology. Oleic acid (OA) and oleyl amine (OLAM) are a common pair used for the synthesis of perovskites. It is well

known that the OA/OLAM pair causes feasible degradation of perovskites through proton exchange under ambient conditions. In addition, the purification process of perovskite NCs causes ligand losses which accelerates the degradation to the non-perovskite  $\delta$ -phase. Generally, organic ligands with a polar head group increase their size in the presence of moisture or polar solvents, leading to detachment from the surface of PeNCs and giving a chance to be replaced by other ligands with comparatively strong interaction with PeNCs. For example, the commonly used OA, O-polar head group has lower interactions compared to the S-head group of other alkyl-polymers. The O-polar ligands are replaced with the S-containing ligands and thus the stability and dispersability of PeNCs are enhanced.<sup>80</sup> Different types of ligands have been exploited either during the

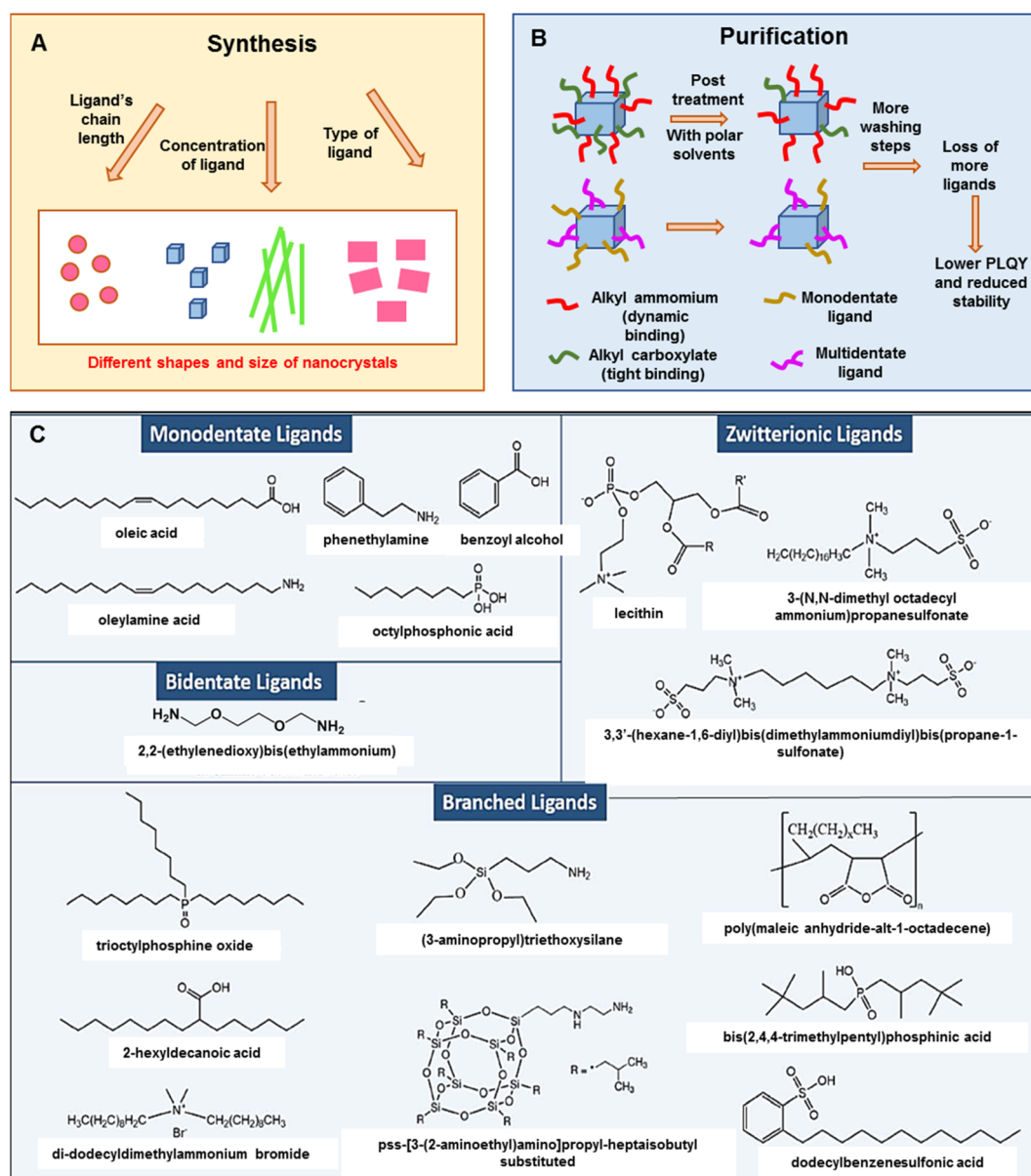


Fig. 3 (A and B) A schematic representation of the role of ligands in the synthesis and purification of PeNCs (modified with permission from ref. 92). (C) Chemical representation of different types of capping ligands used for PeNCs (adopted with permission from ref. 92).

reaction as well as in the post-synthetic treatment.<sup>81–84</sup> It is observed that the ligand chain length, ligand concentration, and molecular structure of the ligand (denticity, linear/branched structure) have direct effects in determining the shape and size of the NCs (Fig. 3A). Bulky ligands have less coverage on the surface, which leads to rapid attachment to the respective facets to form perovskite nanocubes.<sup>85,86</sup> Long-chain alkyl ammonium salts can increase the hydrophobicity and solubility of organic solvents of PeNCs.<sup>87</sup> PeNCs passivated by zwitterionic and bidentate ligands have enhanced colloidal stability, thermal stability as well as moisture stability compared to PeNCs with monodentate ligand caps.<sup>88</sup> Liu *et al.* carried out an in-depth investigation on the roles of organic amines and acids in the ligand-mediated synthesis of colloidal CsPbBr<sub>3</sub> NCs. They discovered that ammonium ions can lead to the growth of anisotropic nanoplatelets and carboxylate ligands are essential for the size-tunability of isotropic nanocubes.<sup>89</sup> During the purification process of perovskite NCs, ligands are detached from the surface of the NCs which causes low colloidal stability and thus a lengthy washing step is not desirable (Fig. 3B).

High-density insulating ligand passivation deteriorates optoelectronic properties; hence different types of ligands have been explored to balance between stability and optoelectronic performance. Surfactants (didodecyltrimethylammonium sulfide (DDA<sup>+</sup>S<sup>2-</sup>),<sup>81</sup> sodium dodecyl sulfate (SDS),<sup>82</sup> dodecylbenzenesulfonic acid (DBSA),<sup>90</sup> *etc.*), bi-dentate ligands (succinic acid, 2,2'-iminodibenzoic acid,<sup>83</sup> N1,N2-didodecyl-N1,N1,N2,N2-tetramethylethane-1,2-diaminium bromide (DTDB),<sup>91</sup> *etc.*), branched ligands,<sup>84,92</sup> and zwitterionic ligands<sup>84,93</sup> have been proved to enhance the ambient stability of PeNCs (Fig. 3C). Branched or zwitterionic ligands have an additional advantage on the smaller and mono-dispersed size distribution of PeNCs especially due to the presence of substantial steric hindrance.<sup>94,95</sup> Additionally, zwitterionic ligand-capped PeNCs often reduce the tedious purification process and form highly packed films with high PLQY and have good stability compared to straight-chain ligands.<sup>94</sup> Furthermore, the perovskites can even be sheltered from water by bidentate ligands that link with one another between molecules. For example, Nag *et al.* demonstrated that long-range cation-stacking is one method by which aromatic diamine ligands like 4,4'-trimethylenedipyridine shield perovskites from water.<sup>96</sup> They have shown that there was no difference in PL after keeping in water for six months. Similarly, Huang *et al.* reported that silane ligands like 3-aminopropyl triethoxysilane (APTES) form a cross-linking matrix by hydrolyzing the silyl ether groups. The APTES ligand effectively protected the perovskite from humidity and increased the resistance to UV and polar solvents.<sup>97</sup> Recently, Shu *et al.* synthesized CsPbBr<sub>3</sub> NCs with high PL intensity through the modified ligand-assisted reprecipitation in which an amphiphilic polymer ligand, octylamine-modified polyacrylic acid (OPA), was used for the synthesis. The PLQY of the OPA-capped CsPbBr<sub>3</sub> NCs remained at 80% of the initial value in water for 15 days.<sup>98</sup> Kim *et al.* proposed a new strategy to synthesize stable PeNCs by controlling the peripheral layer of the octahedral perovskite

geometry.<sup>99</sup> A series of rod-shaped fluorescent hybrid perovskites were synthesized under both acidic and basic conditions without using any capping ligands. They claimed that lead bromide perovskites were stable for up to 6 months underwater without any structural change. Even though there has been significant stability improvement in bromide-based perovskites, there have been almost no reports on water-stable iodide-based perovskites because they are very prone to degradation compared to bromide-based perovskites.

## 4. Novel passivation approaches to achieving water stability

There have been significant efforts made to advance passivation of PeNCs for improved water stability,<sup>100–102</sup> which include inserting the NCs in pores in a porous matrix, embedding in a polymer matrix or in a glass matrix, creating an inorganic coating layer, and superhydrophobic/superhydrophilic functionalization (Fig. 4).<sup>103–105</sup> A large density of defect states inside the energy bandgap of conventional semiconductors can function as trapping states which originate from the corresponding structural defects. Brandt *et al.* explained the defect tolerance of halide perovskites in their electronic structures.<sup>106</sup> They revealed that intrinsic defects generating from the vacancies or interstitial atoms appear as resonances inside the bands; therefore, the surface states are unlikely to develop the intragap states. It means that it is not strictly necessary to use surface ligands or other forms of electronic surface passivation to maintain the purity of the energy bandgap and high PLQY.<sup>107</sup> On the basis of this theoretical prediction, various synthetic approaches have been developed for high-performance stable PeNCs.

### 4.1. Surface passivation by using a porous matrix

Various species of porous matrices (*e.g.*, mesoporous silica, zeolites, molecular sieves, porous polymeric frameworks *etc.*) have provided promise for the synthesis of water-stable PeNCs. The porous matrix acts as a template to confine PeNCs inside and keep them intact with water molecules.<sup>108,109</sup> Superhydrophobic modification can further enhance the aqueous stability of PeNCs. Recently, Xuan *et al.* developed water-stable Sr<sup>2+</sup>-doped CsPbBr<sub>3</sub> which was encapsulated by a molecular sieve matrix and PbBr(OH) composite matrix (Fig. 5A).<sup>110</sup> These composites exhibited 75% PLQY and showed high resistance to heat and water. Impressively, they sustained 99.5% of their initial PLQY even after 200 days when submerged in water, and 63.1% when exposed simultaneously to blue light and water. Wang *et al.* used crystalline inorganic zeolites (AlPO-5) as a porous framework where MAPbBr<sub>3</sub> NCs were *in situ* synthesized in the nanopores of zeolite (Fig. 5B).<sup>111</sup> The nanoconfinement substantially reduced the formation of structural defects in the PeNCs and significantly reduced the lattice vibration so that PL could be maintained at 80 °C. Bright green luminescence of the MAPbBr<sub>3</sub>/zeolite composite was sustained for fifteen months under ambient conditions and maintained for two weeks under aqueous conditions. Although the PL

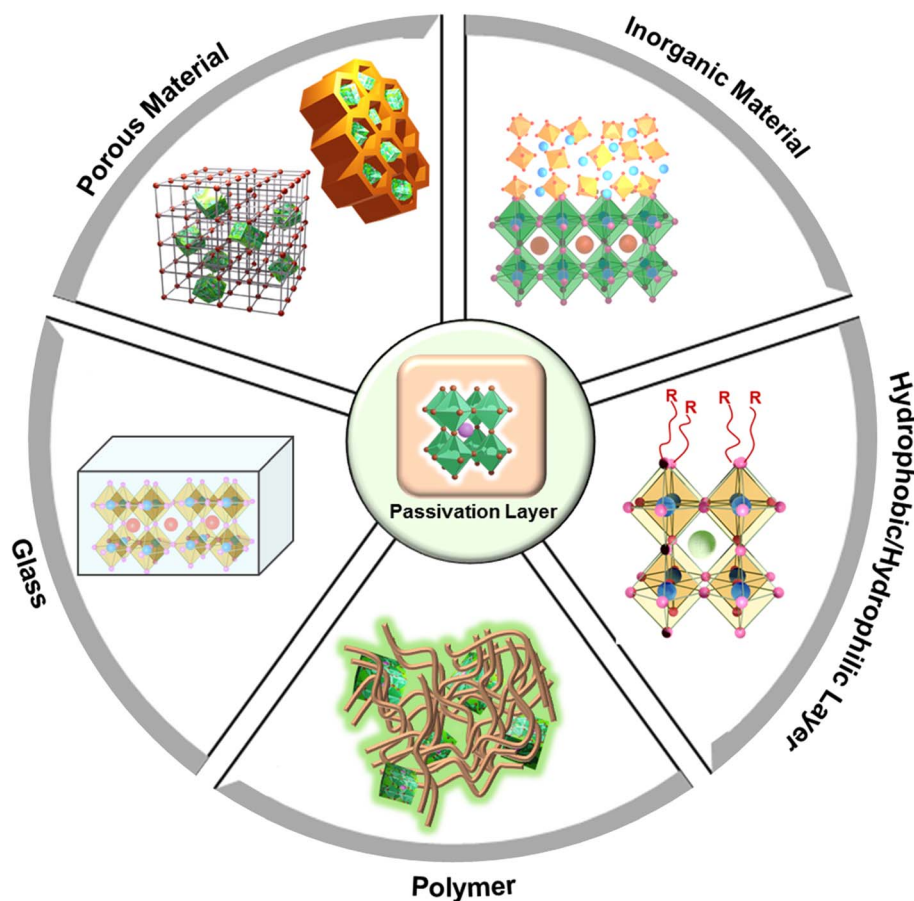


Fig. 4 A schematic representation of the various methods for surface passivation of PeNCs.

intensity of this composite was reduced to 5% of its initial value at 135 °C, PL was gradually restored during the cooling process. Xuan *et al.* demonstrated that porous organic polymeric frameworks also serve as a protection shield to stabilize PeNCs under real-life conditions (Fig. 5C).<sup>107</sup> The organic framework had a hierarchical porous architecture which contained pores ranging from the nano-to micrometer scale. The superhydrophobicity of the organic framework with a water contact angle larger than 150° facilitated selective absorption of CsPbX<sub>3</sub> NCs and made the resultant composite completely phase separated from water (floating on the water phase). Even after 6 months of being submerged in water, this composite sustained its bright luminescence without signs of hydrolytic degradation. In addition, Ma *et al.* fabricated a superhydrophobic polymeric (polydivinylbenzene) porous matrix which provided a confined space to absorb Cs<sub>4</sub>PbBr<sub>6</sub> QDs (Fig. 5D).<sup>112</sup> Initially the composite was non-luminescent; however, the Cs<sub>4</sub>PbBr<sub>6</sub> phase was transformed into a luminescent CsPbBr<sub>3</sub> phase with underwater exposure through the dissolution of CsBr. This structural transformation was reversible, turning back to the non-luminescent Cs<sub>4</sub>PbBr<sub>6</sub> after evaporation of water through the reintegration of CsBr. Here, the superhydrophobic encapsulation prevented the migration of dissolved CsBr, resulting in the stabilization of the CsPbBr<sub>3</sub> phase. It showed high water stability and retained more than 80% of initial PLQY after

prolonged immersion in water for 12 days. The reversible luminescence was used to fabricate an anticounterfeiting device with high-water stability.

#### 4.2. Surface passivation by using inorganic encapsulation

Placing a wide-bandgap inorganic passivation layer on the surface of PeNCs decreased the surface recombination rate of charge carriers and provided durability under harsh environmental conditions.<sup>113</sup> Recently, various types of inorganic passivating materials (SiO<sub>x</sub>, InBr<sub>3</sub>, ZnCl<sub>2</sub>, ZnBr<sub>2</sub>, PbBr<sub>2</sub>, AgNO<sub>3</sub>, BiCl<sub>3</sub>, SnCl<sub>4</sub>, CuBr<sub>2</sub>, *etc.*) have been widely investigated to stabilize PeNCs.<sup>114–117</sup> For instance, Hu *et al.* reported a facile approach to developing a superhydrophobic SiO<sub>x</sub>-coated CsPbBr<sub>3</sub> film by hydrolyzing tetramethyl orthosilicate and then surface-modifying with CH<sub>3</sub>- groups (Fig. 6A).<sup>118</sup> The superhydrophobic perovskite film exhibited good water repellence showing a 25% PL decrease under aqueous conditions for 10 days, self-cleaning characteristics, and enhanced thermal stability at 70 °C. Interestingly, the PL intensity of the film was enhanced by 46% after three months of storage under ambient conditions. XRD spectra and HRTEM images revealed the formation of mixed phases including CsPbBr<sub>3</sub>, CsPb<sub>2</sub>Br<sub>5</sub>, and Pb(OH)Br during the prolonged ambient exposure.

Zhong *et al.* reported the encapsulation of CsPbX<sub>3</sub> NCs with inorganic pyrophosphate (NH<sub>4</sub>AlP<sub>2</sub>O<sub>7</sub>) (Fig. 6B).<sup>119</sup> One of the



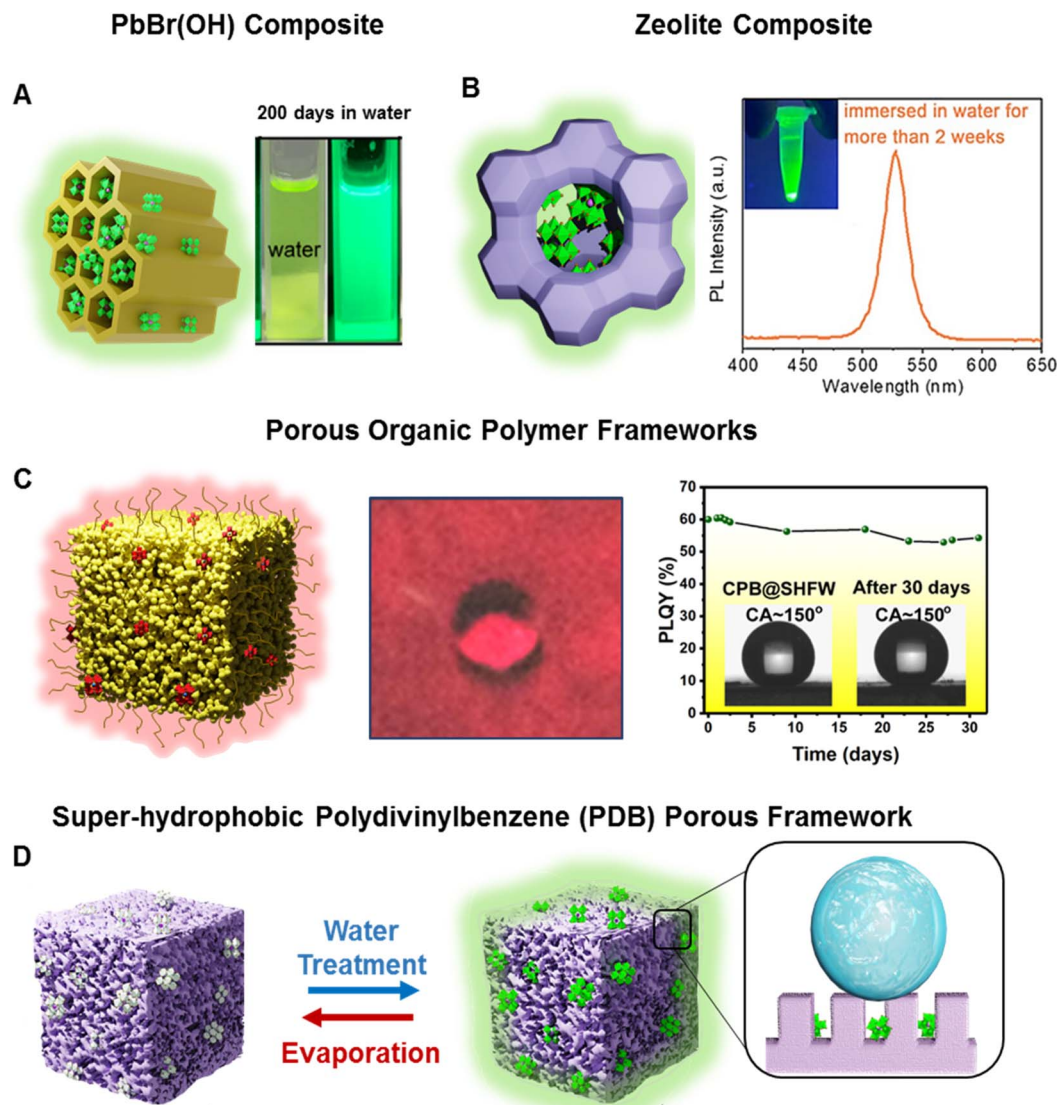


**Fig. 5** Passivation in a porous matrix. (A) Scheme of the  $\text{Sr}^{2+}$ -doped  $\text{CsPbBr}_3$ /molecular sieve/ $\text{PbBr(OH)}$  composite and digital image after being stored for 200 days in an aqueous solution (modified with permission from ref. 110). (B) Scheme of the zeolite/perovskite composite and its PL spectra after being immersed in water for more than 2 weeks (modified with permission from ref. 111). (C) Scheme of the porous organic polymeric frameworks embedded with  $\text{CsPbX}_3$  NCs, digital image of beaded water drops on the composite films, graph representing the change in photoluminescence quantum yield (PLQY) of the composite in the water medium (inset: the CA pictures before and after being submerged in water for 31 days) (modified with permission from ref. 107). (D) Scheme of the PeNCs embedded in the super-hydrophobic polydivinylbenzene (PDB) porous framework. The non-luminescent  $\text{Cs}_4\text{PbBr}_6$  and luminous  $\text{CsPbBr}_3$  were reversible by alternating water treatment and drying (modified with permission from ref. 112).

important requirements for the inorganic passivation layer is the strong interactions between the perovskite surface and passivation layer so that it can be sustained under harsh environmental conditions. Density functional theory (DFT) calculation confirmed the formation of a strong Pb–O bond between the  $\text{P}_2\text{O}_7^{4-}$  group and the Pb atom in  $\text{CsPbBr}_3$ . The strong bond provided remarkable stability against water, heat, and UV irradiation. Interestingly, pyrophosphate-encapsulated  $\text{CsPbBr}_3$  could make highly stable dispersion in a water medium due to its negative zeta potential ( $-30.2$  mV). The PL intensity of their aqueous dispersion remained intact even after storing for 400 days. Moreover, the dispersed composite material retained its

PL even in extremely acidic (pH 2.0) and basic (pH 12.5) solutions after 400 days. The core–shell encapsulation protected the PeNCs from heat deterioration and UV light-induced degradation. This highly stable aqueous dispersion was used in high-resolution inkjet printing on paper which was kept in an aqueous medium for 100 days without any noticeable loss of PL intensity and any trace of lead leakage. Water-insoluble lead salts such as  $\text{PbSO}_4$ ,  $\text{PbCO}_3$ , and  $\text{Pb}_3(\text{PO}_4)_2$  have been used for surface passivation in perovskite-based solar cells. Although hydration and dissolution in an aqueous medium are the main reasons for the PeNC degradation, the lead(II) oxy salt layer was robust enough to prevent water from permeating into the



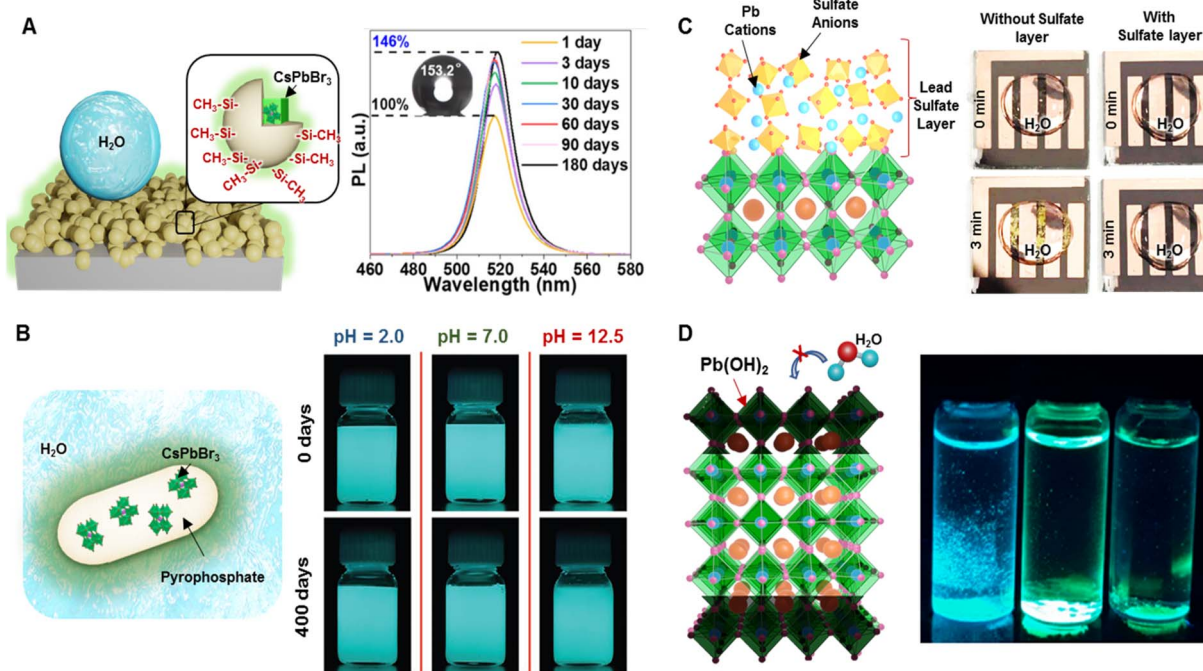


Fig. 6 Surface passivation by inorganic encapsulation. (A) Scheme illustrating the film of the superhydrophobic  $\text{SiO}_2$ -encapsulated  $\text{CsPbBr}_3$  composite and PL spectra of the composite film at various time points after being stored in an ambient environment, (inset: water contact angle of the water droplet on the composite film after 3 months of storage in the ambient atmosphere) (modified with permission from ref. 118). (B) Scheme of the encapsulated  $\text{CsPbBr}_3$  nanocrystal with inorganic pyrophosphate and a digital image of the composite dispersed in an aqueous solution of different pH (modified with permission from ref. 119). (C) Scheme depicting the top layer of lead sulfate on the perovskite surface as a passivation layer and photographs of the device after being exposed to a water droplet for three minutes without (left) and with (right) the top layer lead sulfate (modified with permission from ref. 113). (D) Scheme showing the formation of the  $\text{Pb}(\text{OH})_2$  layer which can protect the PeNCs from water molecules and the digital image of the  $\text{Pb}(\text{OH})_2$  layer coated on different PeNCs after being immersed in water under UV light (modified with permission from ref. 99).

perovskite. For instance, Yang *et al.* developed  $\text{PbSO}_4$  and  $\text{Pb}_3(\text{PO}_4)_2$  layers on perovskite films and demonstrated an enhanced water resistance of the perovskite surface (Fig. 6C).<sup>113</sup> X-ray photoemission spectroscopy measurements and DFT calculation confirmed the strong preferential interaction of  $\text{SO}_4^{2-}$  and  $\text{PO}_4^{3-}$  with Pb atoms of the perovskite surface. When the lead sulfate-coated perovskite device was submerged in water, it remained black instead of turning yellow, which was caused by the formation of  $\text{PbI}_2$ . The coating layer allowed a fast carrier recombination lifetime and increased the solar conversion efficiency up to 21.1%. The solar cell maintained 96.8% of the original efficiency for 1200 h at 65 °C. The formation of the  $\text{Pb}(\text{OH})_2$  layer was also able to stabilize PeNCs. Jana *et al.* reported a simple aqueous synthesis of rod-shaped PeNCs in basic or acidic media where a layer of  $\text{Pb}(\text{OH})_2$  was formed on the surface of perovskites as confirmed by XRD and TEM analysis (Fig. 6D).<sup>99</sup> The  $\text{Pb}(\text{OH})_2$  layer effectively prevented water diffusion into the perovskite, thus retaining the PL intensity even when immersed in water over 6 months.

#### 4.3. Passivation by post-treatment with a hydrophobic/hydrophilic organic layer

Degradation of PeNCs is usually initiated from the defect sites in the grain boundaries and surfaces. These defects are reactive towards oxygen and water which makes them vulnerable even

under ambient conditions.<sup>120</sup> Recently, various electron-donating hydrophobic molecules have been investigated to effectively reduce the defect-nucleating sites or heal the existing defects on perovskite films, which has been performed by chemically binding organic molecules on the undercoordinated lead ion sites (Fig. 7A).<sup>36</sup> Mathews *et al.* demonstrated that passivating the perovskite surface and grain boundaries with hydrophobic pentafluoropropyl ammonium iodide could improve the device efficiency by reducing charge carrier recombination and increasing its lifetime.<sup>121</sup> This passivated perovskite solar cell exhibited remarkable stability under ambient conditions for 169 days without any structural change and maintained above 95% of its initial efficiency. Superhydrophobic modification could further improve the water stability of PeNCs.<sup>122–124</sup> For instance, Zhang *et al.* developed a superhydrophobic lead PeNC film by creating a self-assembled monolayer of 1H,1H,2H,2H-perfluorodecanethiol.<sup>36</sup> The thiol group of the perfluorocarbon chains passivated the uncoordinated sites on the perovskite surface by forming the Pb–S bond.

Despite the common belief that the hydrophilic layer can help water penetration, the hydrophilic passivation layer can also improve the stability of the perovskite against moisture (Fig. 7B). For example, Ma *et al.* showed that the post-treatment of a perovskite film with hydroxyl group-containing amine molecules could help to sustain the device efficiency under high

Fig. 7 (A) Schematic diagram representing hydrophobic passivation of the perovskite surface by using different hydrophobic molecules. (B) Schematic representation of the hydrophilic passivation of the perovskite surface utilizing several hydrophilic molecules.

using different polymer solubilities in solvents (Fig. 8A).<sup>133</sup> The perovskite precursors were incorporated inside the polymer matrix when the polymer matrix was swollen in a relatively good solvent. The evaporation of the solvent initiated rapid homogeneous crystallization of the PeNCs in the shrunk polymer matrix. Several polymer matrices have been utilized, but polystyrene, polyvinyl chloride, acrylonitrile butadiene styrene, and polycarbonate polymer composites exhibited superior water stability. The perovskite/polymer composites were kept immersed in water for 120 days with less than a 7% loss in PLQY. On the other hand, *in situ* synthesis of PeNCs has also been conducted by using a UV-curable polymer. For instance, Zhang *et al.* synthesized PeNCs from the precursor absorbed in the photo-polymerizable hydrophobic polyacrylate matrix which improved the protection of the PeNCs from water (Fig. 8B).<sup>40</sup> Owing to low water permeability and high chemical durability of the polyacrylate matrix, the perovskite/polymer matrix survived in harsh aqueous media in pH 2 to pH 12. The lead leakage in an aqueous medium was significantly reduced, allowing for its usage in biomedical applications. Wang *et al.* employed two-dimensional silica nanosheets as nanoreactors in

which a hydrophobic poly(acrylic acid)-*block*-polystyrene brush was grafted (Fig. 8C).<sup>134</sup> The polymer brush produced a thick hydrophobic barrier. The brush collapsed when it came into contact with water molecules due to their hydrophobicity.

Modification by post-synthesis treatment has also been investigated. In this method, photo-crosslinking of the unsaturated hydrocarbon ligands on the PeNC surfaces has been used to develop water-stable uniform PeNCs and a polymer composite layer. For example, Park *et al.* reported a novel method for improving perovskite stability by using 4-vinylbenzyl-dimethyl octadecyl ammonium chloride as a photo-crosslinkable and polymerizable ligand (Fig. 8D).<sup>135</sup> The ammonium sites of the ligand enabled adequate ionic interaction with the perovskite surface, the styryl group enabled the crosslinking of two neighbouring nanocrystals through radical polymerization, and the alkyl side chain provided the hydrophobic protection to enhance resistance to hydrolytic degradation. Similarly, Sun *et al.* also used 4-vinylbenzyl-dimethyloctadecylammonium chloride as a photo-crosslinkable ligand for MAPbBr<sub>3</sub>. This composite showed no significant change in PL intensity after prolonged water

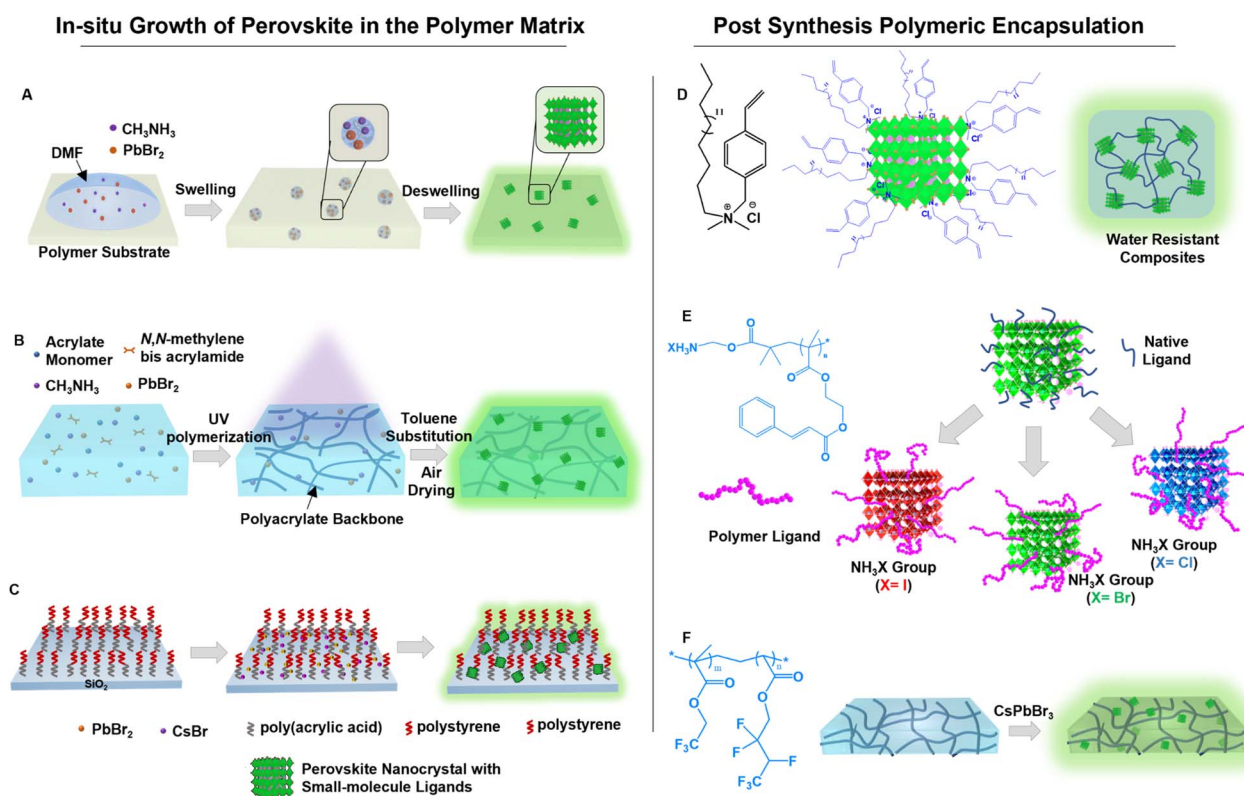


Fig. 8 Passivation by embedding in the polymer matrix. (A) Scheme representing the swelling–deswelling approach for the *in situ* growth of PeNCs in the polymer matrix (modified with permission from ref. 133). (B) Scheme depicting the synthesis of PeNCs inside the photo-polymerizable hydrophobic polyacrylate matrix (modified with permission from ref. 40). (C) Scheme illustrating hydrophobic two-dimensional silica nanosheets grafted with poly(acrylic acid)-*block*-polystyrene. The nanosheets were used as nanoreactors for *in situ* synthesis of PeNCs (modified with permission from ref. 134). (D) Scheme of the post-synthesis using 4-vinylbenzyl-dimethyl octadecyl ammonium chloride as a photo-crosslinkable and polymerizable ligand onto PeNCs (modified with permission from ref. 135). (E) Scheme of post-encapsulation of PeNCs with ammonium halide-terminated poly(2-cinnamoyloxyethylmethacrylate) (modified with permission from ref. 42). (F) Scheme representing a self-healable hydrophobic elastomer with dipole–dipole interaction used for post-synthesis encapsulation of PeNCs (modified with permission from ref. 135).



exposure for 90 days.<sup>136</sup> In another report, Jang *et al.* developed highly water-stable PeNC composites using a UV-induced free-radical reaction of a methacrylate-functionalized matrix resin. This composite could maintain high PLQY ( $\sim 70\%$ ) for more than 600 days in high abrasive liquid medium (*e.g.*, in water, acid and basic solutions, and in different organic solvents).<sup>137</sup> Ligand exchange by long polymer chains has also been successful in passivation. Ko *et al.* reported the ligand exchange by ammonium halide-terminated poly(2-cinnamoylox-ethylmethacrylate) (Fig. 8E).<sup>42</sup> The cinnamoyl group could undergo the UV-induced cycloaddition reaction which significantly reduced lead leakage and increased stability toward diverse polar solvents (such as water or alcohol). Recently, Liu *et al.* used a self-healable hydrophobic fluoroelastomer as the polymer matrix for post-synthesis encapsulation of PeNCs (Fig. 8F), in which the ion-dipole interactions between the positively charged perovskite QDs and the  $\text{CF}_3$  dipoles on the polymers provided excellent compatibility.<sup>138</sup> Moreover, abundant dipole-dipole interactions of  $\text{CF}_3$  groups enabled the underwater healing process of this material. After being submerged for months under a variety of harsh conditions (water, pH 1, pH 7, pH 13, and salty water), the optical and mechanical characteristics of the composite remained intact.

Recently, the encapsulation of PeNCs with block copolymers has been proven to be a potential method to increase stability due to the self-assembly of the polymer chains and the effective interaction between block copolymers and PeNCs. For instance, Zhou *et al.* prepared air- and water-stable stretchable  $\text{MAPbBr}_3$  PeNC composites in the polystyrene-*block*-poly(ethylene butylene)-*block*-polystyrene (SEBS) matrix. The average PL lifetime of the composite varied from 368.3 ns to 599.8 ns before and after being submerged for 70 days in water. However, PL intensity was significantly increased to 225% after 70 days of immersion in water due to the oxidation of Pb atoms which quenched excitons and created the platelet structures with reduced surface defects.<sup>139</sup> Similarly, Park and coworkers

developed a moisture stable  $\text{MAPbX}_3$  NC film by passivating with polystyrene-*block*-poly(2-vinylpyridine).<sup>140</sup> The poly(2-vinylpyridine) chains effectively prohibited water molecules from entering the  $\text{MAPbBr}_3$  NCs. PLQY of this PeNC film remained unaltered at high temperature ( $150^\circ\text{C}$ ) and high RH (70%) for 24 h. As demonstrated by Liu *et al.*,<sup>141</sup> a colloidal solution including  $\text{MAPbBr}_3/\text{SiO}_2$  NCs passivated by starlike trilobe poly(2-hydroxyethyl methacrylate)-*graft*-poly(acrylic acid)-*block*-polystyrene (partially crosslinked) exhibited no significant change in the PL emission peak for 300 min in the presence of 20% water. Further, Yang *et al.* reported that  $\text{MAPbBr}_3$  QDs passivated by polystyrene-*block*-poly(ethyl oxide) were stored in an aqueous solution for more than 7 months and exhibited a slight PLQY decrease (from 43% to 33%) and a slight red-shift (1 nm) of the PL emission.<sup>142</sup> In another report, He *et al.* fabricated a  $\text{MAPbBr}_3/\text{SiO}_2$  NC thin film, in which the NCs were capped with polystyrene block copolymers, and showed strong PL intensity after 30 min in water.<sup>143</sup> In another report, Avugadda *et al.* developed the synthesis of PeNCs in the capsules of polystyrene-*block*-poly(acrylic acid). The encapsulated PeNCs retained the initial PLQY (60%) even after being dispersed in water for 2 years.<sup>144</sup>

#### 4.5. Perovskite crystallization in a glass matrix

Encapsulation in glass has been one of the main approaches for the passivation of implantable devices. The perovskite crystallization inside a glass matrix can provide exceptional chemical and physical stability.<sup>145</sup> Laser-induced *in situ* crystallization has been widely employed to produce highly stable 3D perovskite patterns for advanced photonic applications. For instance, Huang *et al.* used femtosecond laser irradiation and thermal annulation to demonstrate reversible encryption by creating 3D perovskite patterns and removing the patterns within the glass matrix (Fig. 9).<sup>41</sup> Here, the femtosecond laser provided an extremely high power density which allowed formation of the  $\text{CsPbBr}_3$  QDs deep inside the glass. By employing a computer-

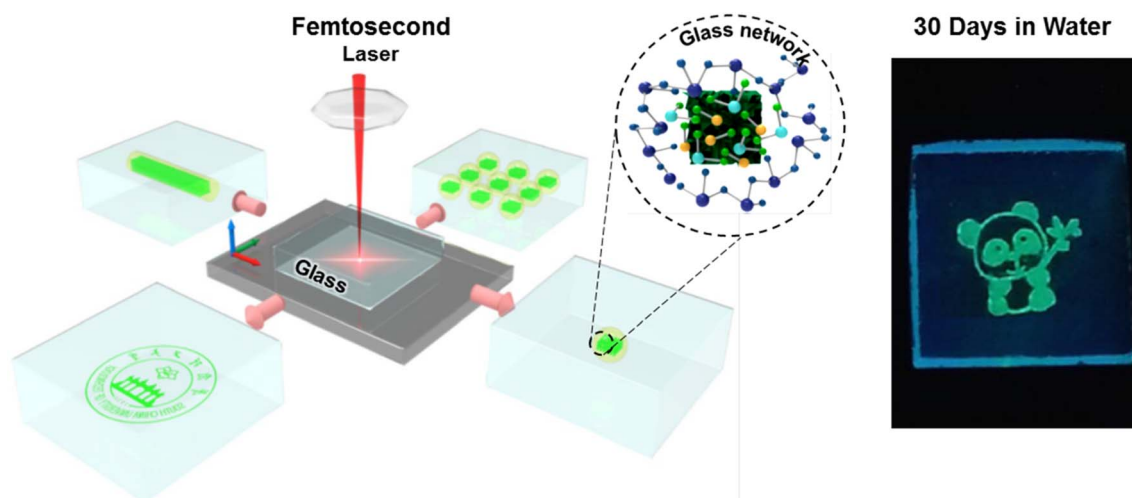


Fig. 9 Scheme of the 3D perovskite patterns generated inside the glass matrix by using femtosecond laser irradiation and the digital image of  $\text{CsPbBr}_3$  patterns after being stored in water for 30 days (modified with permission from ref. 41).



Table 1 Summary of recent progress in moisture or water stability of perovskites adopting different approaches

Perovskite	Passivation agent	Ambient atmosphere	Under water	Under acidic or basic solution	Ref.
Si <sup>2+</sup> doped CsPbBr <sub>3</sub>	Molecular sieve/PbBr(OH) composite matrix	—	99.5% PLQY retention after 200 days	—	110
MAPbBr <sub>3</sub>	Zeolite (AlPO-5) encapsulation	Stable for 15 months	Stable for >2 weeks	—	111
CsPbBr <sub>3</sub>	Superhydrophobic porous polymer matrix	—	Stable for 6 months.	—	107
CsPbBr <sub>3</sub>	Superhydrophobic poly(divinylbenzene) porous matrix	—	>80% PLQY retention after 12 days	—	155
CsPbBr <sub>3</sub>	Silicon-based molecular sieve encapsulation	—	~100% PL retention after 50 days	100% PL retention after 50 days in 1 M HCl solution	156
CsPbBr <sub>3</sub>	Mesoporous SiO <sub>2</sub> encapsulation	—	95% PL retention after 30 days	55% PL retention after 30 days	157
CsPbBr <sub>3</sub>	Superhydrophobic SiO <sub>2</sub> encapsulation	46% PL enhancement after 3 months	75% PL retention after 10 days	—	118
CsPbBr <sub>3</sub>	Inorganic pyrophosphate (NH <sub>4</sub> AlP <sub>2</sub> O <sub>7</sub> ) encapsulation	—	Stable for 400 days	Stable for 400 days (pH 2.0 and 12.5)	119
Cs <sub>0.05</sub> FA <sub>0.81</sub> MA <sub>0.14</sub> PbI <sub>2.55</sub> Br <sub>0.45</sub>	PbSO <sub>4</sub> and Pb <sub>3</sub> (PO <sub>4</sub> ) <sub>2</sub> layers	96.8% PCE retention for 1200 hours at 65 °C	Stable for 3 min	—	113
MAPbBr <sub>3</sub> , MAPbBr <sub>3-x</sub> Cl <sub>x</sub> , CsPbBr <sub>3</sub>	Pb(OH) <sub>2</sub> layer	—	Stable over over 6 months	—	99
FAPbI <sub>3</sub>	Pentafluoropropylammonium iodide layer	95% PCE retention for 169 days	—	—	121
Cs <sub>0.05</sub> (FA <sub>0.85</sub> MA <sub>0.15</sub> ) <sub>0.95</sub> Pb(I <sub>0.85</sub> Br <sub>0.15</sub> ) <sub>3</sub>	Self-assembled monolayers of 1H,1H,2H,2H-Perfluorodecanethiol	100% PCE retention for 7 days at 55% RH	Stable over over 6 months	Stable for 45 s in an acidic solution	36
(FEA) <sub>2</sub> PbI <sub>4</sub>	Pentafluorophenylethyl ammonium (FEA) lead iodide bilayer	90% PCE retention after 1000 h at 40% RH	—	—	78
FAPbI <sub>3</sub>	Hydroxyl group-containing amine layer	90% PCE retention after 1000 h at 20% RH	—	—	125
MAPbI <sub>3</sub>	Hygroscopic poly(ethylene glycol) (PEG) layer	Stable for 15 days at 88% RH	—	—	126
FA <sub>0.85</sub> MA <sub>0.15</sub> PbI <sub>3</sub>	Hydrophilic sorbitan monolaurate molecules layer	90% PCE retention after 29 days at 80% RH	Stable for six h	—	127
MAPbBr <sub>3</sub>	Polystyrene, polyvinyl chloride, acrylonitrile butadiene styrene, and polycarbonate polymer encapsulation	Stable for 5 months	<7% loss in PLQY after 120 days	—	133
MAPbBr <sub>3</sub>	Hydrophobic polyacrylate matrix	—	Stable for 110 days	Stable for 16 days (pH 2 and 12)	40

Table 1 (Contd.)

Perovskite	Passivation agent	Ambient atmosphere	Under water	Under acidic or basic solution	Ref.
CsPbBr <sub>3</sub>	Hydrophobic poly(acrylic acid)- <i>block</i> -polystyrene grafted two-dimensional silica nanosheets	>95.5% PL retention after 60 days	Maintained 81.8% of emission after 24 h	—	134
MAPbBr <sub>3</sub>	4-Vinyl-benzyl-dimethyl octadecyl ammonium chloride as a photo-cross-linkable and polymerizable ligand encapsulation	Stable for more than 100 days	Stable for more than 100 days	Stable for more than 100 days (pH 1 and pH 13)	135
CsPbBr <sub>3</sub>	Post-encapsulation with ammonium halide-terminated poly(2-cinnamoyloxyethylmethacrylate)	Stable for 20 days.	Maintaining 60% of its initial PL over a week	—	42
CsPbBr <sub>3</sub>	Post-synthesis encapsulation with fluorine elastomer	—	Stable for 30 days	Stable for 30 days (pH 1 and pH 13)	78
CsPbBr <sub>3</sub>	Glass matrix encapsulation	—	Stable for 90 days	—	41

controlled stage, this method also made it possible to print complicated three-dimensional patterns. The size and luminescence intensity of the CsPbBr<sub>3</sub> QDs could be tuned by adjusting the laser exposure time, laser power density, and moving speed of the sample stage. No discernible loss of PL intensity was observed in ethanol and deionized water for 90 days. Similarly to this work, Dong *et al.* fabricated CsPb(Cl/Br)<sub>3</sub> patterns within a borosilicate glass by using femtosecond laser irradiation and subsequent low-temperature thermal treatment.<sup>146</sup> Femtosecond laser irradiation assisted localized collapse of the glass matrix which enabled the atoms to migrate into the glass and form crystal nuclei. The nuclei grew into PeNCs during heat treatment at 400 °C. The laser-printed PeNC patterns remained intact even after a month of immersion in deionized water.

## 5. Conclusion and outlook

The superior optoelectronic properties of the halide PeNCs necessitate moisture stability for practical applications. We have summarized the synthetic strategies to obtain water stability without degrading their intrinsic optical properties. Hydrocarbons such as polymers, ligands, or mesoporous hydrophobic organic frameworks have been intensively employed to achieve remarkable underwater stability. In Table 1, we have summarized recent progress in the synthesis of water-stable PeNCs by employing different approaches.

Although the use of long-chain organic hydrocarbons or mesoporous organic/inorganic frameworks drastically improves the optical stability of PeNCs, optoelectronic or electronic applications are difficult due to their insulating nature. Adopting an extremely thin organic/inorganic insulating layer that allows electron tunneling but prevents water penetration, is a promising research direction. Commercial products needed a balance between water stability and optoelectronic performance to explore optimal conditions for target applications. It has been demonstrated that adding conductive conjugated polymers<sup>147,148</sup> (such as PEDOT<sup>149</sup> and P3HT<sup>150</sup>) increases stability, passivates surfaces, and increases intrinsic conductivity. Future research can concentrate on the synthesis of conducting polymer-coated perovskite NCs to enhance the transport characteristics in the films which is rarely explored. Since the encapsulated PeNCs offer down-conversion of light from LEDs, they may be used for conventional displays as a color filter layer. To date, the majority of research studies using the passivated PeNCs have been devoted to centimetre-scale devices or simple-structured optical uses.<sup>151,152</sup> Therefore, future research might concentrate on creating large-area devices that are stable over time even under extremely robust conditions.

Other future aspects of the polymer/perovskite composite are to study the precise mechanisms of how the polymer interacts with PeNCs and how it depends upon the terminal functional groups and the surface energy of the polymers. It is also necessary to clarify how polymer chain packing and composition affect the water/oxygen transport as well as the overall contribution of the polymers to the electrical band

structure.<sup>130,131</sup> The production of PNC/polymer nanocomposites with improved characteristics and the comprehension of polymer–PNC interactions could benefit from computational modelling. Lead toxicity of perovskites is one of the big concerns, so far Sn<sup>II</sup>, Sn<sup>IV</sup>, Sb<sup>III</sup>, Bi<sup>III</sup>, Pd<sup>IV</sup>, Cu<sup>II</sup>, In<sup>III</sup>, and Ag<sup>I</sup> have been used to replace the Pb-counter part.<sup>153</sup> Nonetheless, polymer composites with lead-free perovskite nanostructures are still in the beginning stage and need more attention. Another, upcoming hot topic is polymer-directed or guided self-assembly of PeNCs to improve their optical and electrical properties along with desired stability in water. Using self-assembly techniques, the morphology of the perovskites may be fine-tuned.<sup>154</sup>

## Conflicts of interest

The authors declare no competing financial interest.

## Acknowledgements

This work was supported by the National Research Foundation of Korea grant NRF-2022M3H4A1A02074314.

## References

- Z. Ji, Y. Liu, M. Yao, Z. Zhang, J. Zhong and W. Mai, *Adv. Funct. Mater.*, 2021, **31**, 2104320.
- A. P. Litvin, X. Zhang, E. v. Ushakova and A. L. Rogach, *Adv. Funct. Mater.*, 2021, **31**, 2010768.
- T. Dey, A. Ghorai, S. Das and S. K. Ray, *Nanotechnology*, 2023, **34**, 065201.
- M. D. Irwin and V. V. Dhas, *US Pat.*, US010333082B2, 2019.
- T.-W. Lee, S. Im, Y.-H. Kim and H. Cho, *US Pat.*, US10193088B2, 2019.
- Y.-H. Kim, J. Park, S. Kim, J. S. Kim, H. Xu, S.-H. Jeong, B. Hu and T.-W. Lee, *Nat. Nanotechnol.*, 2022, **17**, 590–597.
- H. Snaith and M. Lee, *US Pat.*, US010079320B2, 2018.
- S. Mahato, A. Ghorai, S. K. Srivastava, M. Modak, S. Singh and S. K. Ray, *Adv. Energy Mater.*, 2020, **10**, 2001305.
- J. Jeong, M. Kim, J. Seo, H. Lu, P. Ahlawat, A. Mishra, Y. Yang, M. A. Hope, F. T. Eickemeyer, M. Kim, Y. J. Yoon, I. W. Choi, B. P. Darwich, S. J. Choi, Y. Jo, J. H. Lee, B. Walker, S. M. Zakeeruddin, L. Emsley, U. Rothlisberger, A. Hagfeldt, D. S. Kim, M. Grätzel and J. Y. Kim, *Nature*, 2021, **592**, 381–385.
- A. Al-Ashouri, E. Köhnen, B. Li, A. Magomedov, H. Hempel, P. Caprioglio, J. A. Márquez, A. B. Morales Vilches, E. Kasparavicius, J. A. Smith, N. Phung, D. Menzel, M. Grischek, L. Kegelman, D. Skroblin, C. Gollwitzer, T. Malinauskas, M. Jošt, G. Matič, B. Rech, R. Schlattmann, M. Topič, L. Korte, A. Abate, B. Stannowski, D. Neher, M. Stolterfoht, T. Unold, V. Getautis and S. Albrecht, *Science*, 1979, **2020**(370), 1300–1309.
- J. M. Luther, A. Swarnkar, A. R. Marshall and E. M. Sanehira, *US Pat.*, US010273403B2, 2019.
- Y. Liu, Y. Dong, T. Zhu, D. Ma, A. Proppe, B. Chen, C. Zheng, Y. Hou, S. Lee, B. Sun, E. H. Jung, F. Yuan, Y. Wang, L. K. Sagar, S. Hoogland, F. P. García de Arquer, M.-J. Choi, K. Singh, S. O. Kelley, O. Voznyy, Z.-H. Lu and E. H. Sargent, *J. Am. Chem. Soc.*, 2021, **143**, 15606–15615.
- A. Fakharuddin, M. K. Gangishetty, M. Abdi-Jalebi, S.-H. Chin, A. R. bin Mohd Yusoff, D. N. Congreve, W. Tress, F. Deschler, M. Vasilopoulou and H. J. Bolink, *Nat. Electron.*, 2022, **5**, 203–216.
- K. Lin, C. Yan, R. P. Sabatini, W. Feng, J. Lu, K. Liu, D. Ma, Y. Shen, Y. Zhao, M. Li, C. Tian, L. Xie, E. H. Sargent and Z. Wei, *Adv. Funct. Mater.*, 2022, **32**, 2200350.
- S. Pal, A. Ghorai, D. K. Goswami and S. K. Ray, *Nano Energy*, 2021, **87**, 106200.
- J. S. Kim, J.-M. Heo, G.-S. Park, S.-J. Woo, C. Cho, H. J. Yun, D.-H. Kim, J. Park, S.-C. Lee, S.-H. Park, E. Yoon, N. C. Greenham and T.-W. Lee, *Nature*, 2022, **611**, 688–694.
- J.-M. Heo, H. Cho, S.-C. Lee, M.-H. Park, J. S. Kim, H. Kim, J. Park, Y.-H. Kim, H. J. Yun, E. Yoon, D.-H. Kim, S. Ahn, S.-J. Kwon, C.-Y. Park and T.-W. Lee, *ACS Energy Lett.*, 2022, **7**, 2807–2815.
- G. Xiong, Y. Jin, K. Deng, L. Yuan, H. Wu, G. Ju, L. Chen and Y. Hu, *J. Mater. Chem. C*, 2022, **10**, 12316–12322.
- J. Jiang, X. Sun, X. Chen, B. Wang, Z. Chen, Y. Hu, Y. Guo, L. Zhang, Y. Ma, L. Gao, F. Zheng, L. Jin, M. Chen, Z. Ma, Y. Zhou, N. P. Padture, K. Beach, H. Terrones, Y. Shi, D. Gall, T.-M. Lu, E. Wertz, J. Feng and J. Shi, *Nat. Commun.*, 2019, **10**, 4145.
- R. Dong, Y. Fang, J. Chae, J. Dai, Z. Xiao, Q. Dong, Y. Yuan, A. Centrone, X. C. Zeng and J. Huang, *Adv. Mater.*, 2015, **27**, 1912–1918.
- N. B. Kotadiya, P. W. M. Blom and G.-J. A. H. Wetzelaer, *Nat. Photonics*, 2019, **13**, 765–769.
- L. Kong, X. Zhang, C. Zhang, L. Wang, S. Wang, F. Cao, D. Zhao, A. L. Rogach and X. Yang, *Adv. Mater.*, 2022, **34**, 2205217.
- Y. Zhou, I. Poli, D. Meggiolaro, F. de Angelis and A. Petrozza, *Nat. Rev. Mater.*, 2021, **6**, 986–1002.
- Y. Dong, Y. Wang, S.-T. Wu, J. He, H. Chen and J. Chen, *US Pat.*, US20180010039A1, 2018.
- W. Xiang, S. Liu and W. Tress, *Energy Environ. Sci.*, 2021, **14**, 2090–2113.
- S. Cheng and H. Zhong, *J. Phys. Chem. Lett.*, 2022, **13**, 2281–2290.
- J. Li, H.-L. Cao, W.-B. Jiao, Q. Wang, M. Wei, I. Cantone, J. Lü and A. Abate, *Nat. Commun.*, 2020, **11**, 310.
- A. Ghorai, A. Midya and S. K. Ray, *ACS Omega*, 2019, **4**, 12948–12954.
- S. Mahato, A. Ghorai, A. Mondal, S. K. Srivastava, M. Modak, S. Das and S. K. Ray, *ACS Appl. Mater. Interfaces*, 2022, **14**, 9711–9723.
- U.-G. Jong, C.-J. Yu, G.-C. Ri, A. P. McMahon, N. M. Harrison, P. R. F. Barnes and A. Walsh, *J. Mater. Chem. A*, 2018, **6**, 1067–1074.
- Z. Li, M. Yang, J.-S. Park, S.-H. Wei, J. J. Berry and K. Zhu, *Chem. Mater.*, 2016, **28**, 284–292.

- 32 M. M. Byranvand, C. Otero-Martínez, J. Ye, W. Zuo, L. Manna, M. Saliba, R. L. Z. Hoyer and L. Polavarapu, *Adv. Opt. Mater.*, 2022, **10**, 2200423.
- 33 D. W. Ferdani, S. R. Pering, D. Ghosh, P. Kubiak, A. B. Walker, S. E. Lewis, A. L. Johnson, P. J. Baker, M. S. Islam and P. J. Cameron, *Energy Environ. Sci.*, 2019, **12**, 2264–2272.
- 34 W. Zhou, L. Jia, M. Chen, X. Li, Z. Su, Y. Shang, X. Jiang, X. Gao, T. Chen, M. Wang, Z. Zhu, Y. Lu and S. Yang, *Adv. Funct. Mater.*, 2022, **32**, 2201374.
- 35 X. Zhang, W. Zhou, X. Chen, Y. Chen, X. Li, M. Wang, Y. Zhou, H. Yan, Z. Zheng and Y. Zhang, *Adv. Energy Mater.*, 2022, **12**, 2201105.
- 36 H. Zhang, K. Li, M. Sun, F. Wang, H. Wang and A. K.-Y. Jen, *Adv. Energy Mater.*, 2021, **11**, 2102281.
- 37 Z. Li, Z. Zhang, R. Nie, C. Li, Q. Sun, W. Shi, W. Chu, Y. Long, H. Li and X. Liu, *Adv. Funct. Mater.*, 2022, **32**, 2112553.
- 38 G.-Y. Qiao, D. Guan, S. Yuan, H. Rao, X. Chen, J.-A. Wang, J.-S. Qin, J.-J. Xu and J. Yu, *J. Am. Chem. Soc.*, 2021, **143**, 14253–14260.
- 39 Q. Cao, Y. Li, H. Zhang, J. Yang, J. Han, T. Xu, S. Wang, Z. Wang, B. Gao, J. Zhao, X. Li, X. Ma, S. M. Zakeeruddin, W. E. I. Sha, X. Li and M. Grätzel, *Sci. Adv.*, 2021, **7**, eabg0633.
- 40 Y. Zhang, Y. Zhao, D. Wu, J. Xue, Y. Qiu, M. Liao, Q. Pei, M. S. Goorsky and X. He, *Adv. Mater.*, 2019, **31**, 1902928.
- 41 X. Huang, Q. Guo, D. Yang, X. Xiao, X. Liu, Z. Xia, F. Fan, J. Qiu and G. Dong, *Nat. Photonics*, 2020, **14**, 82–88.
- 42 J. Ko, K. Ma, J. F. Joung, S. Park and J. Bang, *Nano Lett.*, 2021, **21**, 2288–2295.
- 43 R. T. Wang, A. F. Xu, W. Li, Y. Li and G. Xu, *J. Phys. Chem. Lett.*, 2021, **12**, 5332–5338.
- 44 A. A. Babaryk, Y. Pérez, M. Martínez, M. E. G. Mosquera, M. H. Zehender, S. A. Svatek, E. Antolín and P. Horcajada, *J. Mater. Chem. C*, 2021, **9**, 11358–11367.
- 45 W. Zhou, Y. Zhao, C. Shi, H. Huang, J. Wei, R. Fu, K. Liu, D. Yu and Q. Zhao, *J. Phys. Chem. C*, 2016, **120**, 4759–4765.
- 46 A. M. A. Leguy, Y. Hu, M. Campoy-Quiles, M. I. Alonso, O. J. Weber, P. Azarhoosh, M. van Schilfgaarde, M. T. Weller, T. Bein, J. Nelson, P. Docampo and P. R. F. Barnes, *Chem. Mater.*, 2015, **27**, 3397–3407.
- 47 E. Mosconi, J. M. Aspiroz and F. de Angelis, *Chem. Mater.*, 2015, **27**, 4885–4892.
- 48 Z. Song, N. Shrestha, S. C. Watthage, G. K. Liyanage, Z. S. Almutawah, R. H. Ahangharnejhad, A. B. Phillips, R. J. Ellingson and M. J. Heben, *J. Phys. Chem. Lett.*, 2018, **9**, 6312–6320.
- 49 J. A. Christians, P. A. Miranda Herrera and P. v. Kamat, *J. Am. Chem. Soc.*, 2015, **137**, 1530–1538.
- 50 M. A. Haque, A. Syed, F. H. Akhtar, R. Shevate, S. Singh, K.-V. Peinemann, D. Baran and T. Wu, *ACS Appl. Mater. Interfaces*, 2019, **11**, 29821–29829.
- 51 J. Yang, B. D. Siempelkamp, D. Liu and T. L. Kelly, *ACS Nano*, 2015, **9**(2), 1955–1963.
- 52 B. Turedi, K. J. Lee, I. Dursun, B. Alamer, Z. Wu, E. Alarousu, O. F. Mohammed, N. Cho and O. M. Bakr, *J. Phys. Chem. C*, 2018, **122**, 14128–14134.
- 53 Q. Lin, S. Bernardi, B. Shabbir, Q. Ou, M. Wang, W. Yin, S. Liu, A. S. R. Chesman, S. O. Furer, G. Si, N. Medhekar, J. Jasieniak, A. Widmer-Cooper, W. Mao and U. Bach, *Adv. Funct. Mater.*, 2022, **32**, 2109442.
- 54 G. Niu, W. Li, F. Meng, L. Wang, H. Dong and Y. Qiu, *J. Mater. Chem. A*, 2014, **2**, 705–710.
- 55 X. Yu, L. Wu, D. Yang, M. Cao, X. Fan, H. Lin, Q. Zhong, Y. Xu and Q. Zhang, *Angew. Chem., Int. Ed.*, 2020, **59**, 14527–14532.
- 56 B. Akbali, G. Topcu, T. Guner, M. Ozcan, M. M. Demir and H. Sahin, *Phys. Rev. Mater.*, 2018, **2**, 034601.
- 57 G. Niu, W. Li, F. Meng, L. Wang, H. Dong and Y. Qiu, *J. Mater. Chem. A*, 2014, **2**, 705–710.
- 58 T. D. Siegler, W. A. Dunlap-Shohl, Y. Meng, Y. Yang, W. F. Kau, P. P. Sunkari, C. E. Tsai, Z. J. Armstrong, Y.-C. Chen, D. A. C. Beck, M. Meilä and H. W. Hillhouse, *J. Am. Chem. Soc.*, 2022, **144**, 5552–5561.
- 59 B. Chen, S. Wang, Y. Song, C. Li and F. Hao, *Chem. Eng. J.*, 2022, **430**, 132701.
- 60 K. Ho, M. Wei, E. H. Sargent and G. C. Walker, *ACS Energy Lett.*, 2021, **6**, 934–940.
- 61 S. Huang, Z. Li, B. Wang, N. Zhu, C. Zhang, L. Kong, Q. Zhang, A. Shan and L. Li, *ACS Appl. Mater. Interfaces*, 2017, **9**, 7249–7258.
- 62 C. Caddeo, M. I. Saba, S. Meloni, A. Filippetti and A. Mattoni, *ACS Nano*, 2017, **11**, 9183–9190.
- 63 S. Wu, Z. Li, M.-Q. Li, Y. Diao, F. Lin, T. Liu, J. Zhang, P. Tieu, W. Gao, F. Qi, X. Pan, Z. Xu, Z. Zhu and A. K.-Y. Jen, *Nat. Nanotechnol.*, 2020, **15**, 934–940.
- 64 B. Hailegnaw, S. Kirmayer, E. Edri, G. Hodes and D. Cahen, *J. Phys. Chem. Lett.*, 2015, **6**, 1543–1547.
- 65 E. Radicchi, F. Ambrosio, E. Mosconi, A. A. Alasmari, F. A. S. Alasmari and F. de Angelis, *J. Phys. Chem. B*, 2020, **124**, 11481–11490.
- 66 W. Kaiser, D. Ricciarelli, E. Mosconi, A. A. Allothman, F. Ambrosio and F. de Angelis, *J. Phys. Chem. Lett.*, 2022, **13**, 2321–2329.
- 67 A. Aziz, N. Aristidou, X. Bu, R. J. E. Westbrook, S. A. Haque and M. S. Islam, *Chem. Mater.*, 2020, **32**, 400–409.
- 68 A. Kaltzoglou, C. C. Stoumpos, A. G. Kontos, G. K. Manolis, K. Papadopoulos, K. G. Papadokostaki, V. Psycharis, C. C. Tang, Y.-K. Jung, A. Walsh, M. G. Kanatzidis and P. Falaras, *Inorg. Chem.*, 2017, **56**, 6302–6309.
- 69 M. M. Rahman, C. Ge, K. Yoo and J.-J. Lee, *Mater. Today Energy*, 2021, **21**, 100803.
- 70 T. Xu, *US Pat.*, US010388898B2, 2019.
- 71 D. Ghosh, A. R. Smith, A. B. Walker and M. S. Islam, *Chem. Mater.*, 2018, **30**, 5194–5204.
- 72 A. Ghorai, S. Mahato, S. K. Srivastava and S. K. Ray, *Adv. Funct. Mater.*, 2022, **32**, 2202087.
- 73 J.-W. Lee, D.-H. Kim, H.-S. Kim, S.-W. Seo, S. M. Cho and N.-G. Park, *Adv. Energy Mater.*, 2015, **5**, 1501310.



- 74 X. Wu, Y. Jiang, C. Chen, J. Guo, X. Kong, Y. Feng, S. Wu, X. Gao, X. Lu, Q. Wang, G. Zhou, Y. Chen, J. Liu, K. Kempa and J. Gao, *Adv. Funct. Mater.*, 2020, **30**, 1908613.
- 75 L. N. Quan, M. Yuan, R. Comin, O. Voznyy, E. M. Beauregard, S. Hoogland, A. Buin, A. R. Kirmani, K. Zhao, A. Amassian, D. H. Kim and E. H. Sargent, *J. Am. Chem. Soc.*, 2016, **138**, 2649–2655.
- 76 L. Romani, A. Bala, V. Kumar, A. Speltini, A. Milella, F. Fracassi, A. Listorti, A. Profumo and L. Malavasi, *J. Mater. Chem. C*, 2020, **8**, 9189–9194.
- 77 Q. Jiang, D. Rebolgar, J. Gong, E. L. Piacentino, C. Zheng and T. Xu, *Angew. Chem., Int. Ed.*, 2015, **54**, 7617–7620.
- 78 Y. Liu, S. Akin, L. Pan, R. Uchida, N. Arora, J. v. Milić, A. Hinderhofer, F. Schreiber, A. R. Uhl, S. M. Zakeeruddin, A. Hagfeldt, M. I. Dar and M. Grätzel, *Sci. Adv.*, 2019, **5**, eaaw2543.
- 79 G. Grancini, C. Roldán-Carmona, I. Zimmermann, E. Mosconi, X. Lee, D. Martineau, S. Narbey, F. Oswald, F. de Angelis, M. Graetzel and M. K. Nazeeruddin, *Nat. Commun.*, 2017, **8**, 15684.
- 80 J. C. Hamill, O. Romiluyi, S. A. Thomas, J. Cetola, J. Schwartz, M. F. Toney, P. Clancy and Y.-L. Loo, *J. Phys. Chem. C*, 2020, **124**, 14496–14502.
- 81 M. I. Bodnarchuk, S. C. Boehme, S. ten Brinck, C. Bernasconi, Y. Shynkarenko, F. Krieg, R. Widmer, B. Aeschlimann, D. Günther, M. v. Kovalenko and I. Infante, *ACS Energy Lett.*, 2019, **4**, 63–74.
- 82 J. Zhang, C. Yin, F. Yang, Y. Yao, F. Yuan, H. Chen, R. Wang, S. Bai, G. Tu and L. Hou, *J. Phys. Chem. Lett.*, 2021, **12**, 2437–2443.
- 83 Y. Chen, S. R. Smock, A. H. Flintgruber, F. A. Perras, R. L. Brutchey and A. J. Rossini, *J. Am. Chem. Soc.*, 2020, **142**, 6117–6127.
- 84 K. Hills-Kimball, H. Yang, T. Cai, J. Wang and O. Chen, *Adv. Sci.*, 2021, **8**, 2100214.
- 85 Y. Bai, M. Hao, S. Ding, P. Chen and L. Wang, *Adv. Mater.*, 2022, **34**, 2105958.
- 86 J. Khan, X. Zhang, J. Yuan, Y. Wang, G. Shi, R. Patterson, J. Shi, X. Ling, L. Hu, T. Wu, S. Dai and W. Ma, *ACS Energy Lett.*, 2020, **5**, 3322–3329.
- 87 G. Liu, H. Zheng, X. Xu, S. Xu, X. Zhang, X. Pan and S. Dai, *Adv. Funct. Mater.*, 2019, **29**, 1807565.
- 88 F. Krieg, S. T. Ochsenbein, S. Yakunin, S. ten Brinck, P. Aellen, A. Süss, B. Clerc, D. Guggisberg, O. Nazarenko, Y. Shynkarenko, S. Kumar, C.-J. Shih, I. Infante and M. v. Kovalenko, *ACS Energy Lett.*, 2018, **3**, 641–646.
- 89 A. Pan, B. He, X. Fan, Z. Liu, J. J. Urban, A. P. Alivisatos, L. He and Y. Liu, *ACS Nano*, 2016, **10**, 7943–7954.
- 90 Y. Liu, Y. Li, X. Hu, C. Wei, B. Xu, J. Leng, H. Miao, H. Zeng and X. Li, *Chem. Eng. J.*, 2023, **453**, 139904.
- 91 Y. Li, M. Cai, M. Shen, Y. Cai and R.-J. Xie, *J. Mater. Chem. C*, 2022, **10**, 8356–8363.
- 92 F. Haydous, J. M. Gardner and U. B. Cappel, *J. Mater. Chem. A*, 2021, **9**, 23419–23443.
- 93 H. Kim, N. Hight-Huf, J. Kang, P. Bisnoff, S. Sundararajan, T. Thompson, M. Barnes, R. C. Hayward and T. Emrick, *Angew. Chem., Int. Ed.*, 2020, **59**, 10802–10806.
- 94 F. Montanarella, K. M. McCall, K. Sakhatskyi, S. Yakunin, P. Trtik, C. Bernasconi, I. Cherniukh, D. Mannes, M. I. Bodnarchuk, M. Strobl, B. Walfort and M. v. Kovalenko, *ACS Energy Lett.*, 2021, **6**, 4365–4373.
- 95 B. Luo, Y. Pu, S. A. Lindley, Y. Yang, L. Lu, Y. Li, X. Li and J. Z. Zhang, *Angew. Chem.*, 2016, **128**, 9010–9014.
- 96 T. Sheikh, S. Maqbool, P. Mandal and A. Nag, *Angew. Chem., Int. Ed.*, 2021, **60**, 18265–18271.
- 97 H. Huang, W. Zhao, H. Yang, X. Zhang, J. Su, K. Hu, Z. Nie, Y. Li and J. Zhong, *J. Mater. Chem. C*, 2021, **9**, 5535–5543.
- 98 Y. Shu, Y. Wang, J. Guan, Z. Ji, Q. Xu and X. Hu, *Anal. Chem.*, 2022, **94**, 5415–5424.
- 99 A. Jana and K. S. Kim, *ACS Energy Lett.*, 2018, **3**, 2120–2126.
- 100 B. Chen, P. N. Rudd, S. Yang, Y. Yuan and J. Huang, *Chem. Soc. Rev.*, 2019, **48**, 3842–3867.
- 101 Y. Shao, Z. Xiao, C. Bi, Y. Yuan and J. Huang, *Nat. Commun.*, 2014, **5**, 5784.
- 102 A. Abate, M. Saliba, D. J. Hollman, S. D. Stranks, K. Wojciechowski, R. Avolio, G. Grancini, A. Petrozza and H. J. Snaith, *Nano Lett.*, 2014, **14**, 3247–3254.
- 103 Y. Ogomi, A. Morita, S. Tsukamoto, T. Saitho, Q. Shen, T. Toyoda, K. Yoshino, S. S. Pandey, T. Ma and S. Hayase, *J. Phys. Chem. C*, 2014, **118**, 16651–16659.
- 104 J. Kim, A. Ho-Baillie and S. Huang, *Solar RRL*, 2019, **3**, 1800302.
- 105 L. Romani, A. Speltini, F. Ambrosio, E. Mosconi, A. Profumo, M. Marelli, S. Margadonna, A. Milella, F. Fracassi, A. Listorti, F. de Angelis and L. Malavasi, *Angew. Chem., Int. Ed.*, 2021, **60**, 3611–3618.
- 106 R. E. Brandt, V. Stevanović, D. S. Ginley and T. Buonassisi, *MRS Commun.*, 2015, **5**, 265–275.
- 107 T. Xuan, J. Huang, H. Liu, S. Lou, L. Cao, W. Gan, R.-S. Liu and J. Wang, *Chem. Mater.*, 2019, **31**, 1042–1047.
- 108 L. Wu, Y. Mu, X. Guo, W. Zhang, Z. Zhang, M. Zhang and T. Lu, *Angew. Chem.*, 2019, **131**, 9591–9595.
- 109 V. Malgras, J. Henzie, T. Takei and Y. Yamauchi, *Angew. Chem., Int. Ed.*, 2018, **57**, 8881–8885.
- 110 T. Xuan, S. Guo, W. Bai, T. Zhou, L. Wang and R.-J. Xie, *Nano Energy*, 2022, **95**, 107003.
- 111 P. Wang, B. Wang, Y. Liu, L. Li, H. Zhao, Y. Chen, J. Li, S. Liu and K. Zhao, *Angew. Chem., Int. Ed.*, 2020, **59**, 23100–23106.
- 112 P. Ma, Y. Hou, Y. Zheng, J. Su, L. Li, N. Liu, Z. Zhang, Y. Ma and Y. Gao, *Chem. Eng. J.*, 2022, **436**, 135077.
- 113 S. Yang, S. Chen, E. Mosconi, Y. Fang, X. Xiao, C. Wang, Y. Zhou, Z. Yu, J. Zhao, Y. Gao, F. de Angelis and J. Huang, *Science*, 1979, **2019**(365), 473–478.
- 114 S. Huang, B. Wang, Q. Zhang, Z. Li, A. Shan and L. Li, *Adv. Opt. Mater.*, 2018, **6**, 1701106.
- 115 Y. Wu, C. Wei, X. Li, Y. Li, S. Qiu, W. Shen, B. Cai, Z. Sun, D. Yang, Z. Deng and H. Zeng, *ACS Energy Lett.*, 2018, **3**, 2030–2037.
- 116 R. K. Behera, S. das Adhikari, S. K. Dutta, A. Dutta and N. Pradhan, *J. Phys. Chem. Lett.*, 2018, **9**, 6884–6891.
- 117 H. Li, Y. Qian, X. Xing, J. Zhu, X. Huang, Q. Jing, W. Zhang, C. Zhang and Z. Lu, *J. Phys. Chem. C*, 2018, **122**, 12994–13000.

- 118 Y. Hu, S. Kareem, H. Dong, W. Xiong, S. Tian, J. Shamsi, L. Li, X. Zhao and Y. Xie, *ACS Appl. Nano Mater.*, 2021, **4**, 6306–6315.
- 119 Q. Zhong, X. Wang, M. Chu, Y. Qiu, D. Yang, T. Sham, J. Chen, L. Wang, M. Cao and Q. Zhang, *Small*, 2022, **18**, 2107548.
- 120 M. I. Saidaminov, J. Kim, A. Jain, R. Quintero-Bermudez, H. Tan, G. Long, F. Tan, A. Johnston, Y. Zhao, O. Voznyy and E. H. Sargent, *Nat. Energy*, 2018, **3**, 648–654.
- 121 K. M. M. Salim, T. M. Koh, D. Bahulayan, P. C. Harikesh, N. F. Jamaludin, B. Febriansyah, A. Bruno, S. Mhaisalkar and N. Mathews, *ACS Energy Lett.*, 2018, **3**, 1068–1076.
- 122 S. Ruidas, A. Das, S. Kumar, S. Dalapati, U. Manna and A. Bhaumik, *Angew. Chem., Int. Ed.*, 2022, **61**, e202210507.
- 123 A. Shome, A. Das and U. Manna, *Chem. Mater.*, 2021, **33**, 8941–8959.
- 124 M. Dhar, A. Das, A. Shome, A. Borbora and U. Manna, *Mater. Horiz.*, 2021, **8**, 2717–2725.
- 125 C. Ma and N.-G. Park, *ACS Energy Lett.*, 2020, **5**, 3268–3275.
- 126 M. Kim, S. G. Motti, R. Sorrentino and A. Petrozza, *Energy Environ. Sci.*, 2018, **11**, 2609–2619.
- 127 H. Chen, H. Wang, Y. Xue, Q. Ge, Y. Du, J. Yin, B. Yang, S. Yang, X. Liu, M. Cai and S. Dai, *Chem. Eng. J.*, 2022, **450**, 138028.
- 128 F. Li and M. Liu, *J. Mater. Chem. A*, 2017, **5**, 15447–15459.
- 129 S. Liang, M. Zhang, G. M. Biesold, W. Choi, Y. He, Z. Li, D. Shen and Z. Lin, *Adv. Mater.*, 2021, **33**, 2005888.
- 130 Q. A. Akkerman, G. Rainò, M. v. Kovalenko and L. Manna, *Nat. Mater.*, 2018, **17**, 394–405.
- 131 M. Dhar, A. Das, D. Parbat and U. Manna, *Angew. Chem., Int. Ed.*, 2022, **61**, e202116763.
- 132 A. Das and U. Manna, *Nanoscale*, 2020, **12**, 24349–24356.
- 133 Y. Wang, J. He, H. Chen, J. Chen, R. Zhu, P. Ma, A. Towers, Y. Lin, A. J. Gesquiere, S. Wu and Y. Dong, *Adv. Mater.*, 2016, **28**, 10710–10717.
- 134 J. Wang, M. Zhang, Y. Liu, Y. Huang, Y. Zhang, J. Jiang, H. Li, J. Chen and Z. Lin, *Nano Energy*, 2022, **98**, 107321.
- 135 J.-M. Park, J. Park, Y.-H. Kim, H. Zhou, Y. Lee, S. H. Jo, J. Ma, T.-W. Lee and J.-Y. Sun, *Nat. Commun.*, 2020, **11**, 4638.
- 136 H. Sun, Z. Yang, M. Wei, W. Sun, X. Li, S. Ye, Y. Zhao, H. Tan, E. L. Kynaston, T. B. Schon, H. Yan, Z.-H. Lu, G. A. Ozin, E. H. Sargent and D. S. Seferos, *Adv. Mater.*, 2017, **29**, 1701153.
- 137 J. Jang, Y. Kim, S. Park, D. Yoo, H. Cho, J. Jang, H. B. Jeong, H. Lee, J. M. Yuk, C. B. Park, D. Y. Jeon, Y. Kim, B. Bae and T. Lee, *Adv. Mater.*, 2021, **33**, 2005255.
- 138 Y. Liu, T. Chen, Z. Jin, M. Li, D. Zhang, L. Duan, Z. Zhao and C. Wang, *Nat. Commun.*, 2022, **13**, 1338.
- 139 H. Zhou, J. Park, Y. Lee, J. Park, J. Kim, J. S. Kim, H. Lee, S. H. Jo, X. Cai, L. Li, X. Sheng, H. J. Yun, J. Park, J. Sun and T. Lee, *Adv. Mater.*, 2020, **32**, 2001989.
- 140 H. Han, B. Jeong, T. H. Park, W. Cha, S. M. Cho, Y. Kim, H. H. Kim, D. Kim, D. Y. Ryu, W. K. Choi and C. Park, *Adv. Funct. Mater.*, 2019, **29**, 1808193.
- 141 Y. Liu, Z. Wang, S. Liang, Z. Li, M. Zhang, H. Li and Z. Lin, *Nano Lett.*, 2019, **19**, 9019–9028.
- 142 S. Yang, F. Zhang, J. Tai, Y. Li, Y. Yang, H. Wang, J. Zhang, Z. Xie, B. Xu, H. Zhong, K. Liu and B. Yang, *Nanoscale*, 2018, **10**, 5820–5826.
- 143 Y. He, Y. J. Yoon, Y. W. Harn, G. v. Biesold-McGee, S. Liang, C. H. Lin, V. v. Tsukruk, N. Thadhani, Z. Kang and Z. Lin, *Sci. Adv.*, 2019, **5**, eaax442.
- 144 S. K. Avugadda, A. Castelli, B. Dhanabalan, T. Fernandez, N. Silvestri, C. Collantes, D. Baranov, M. Imran, L. Manna, T. Pellegrino and M. P. Arciniegas, *ACS Nano*, 2022, **16**, 13657–13666.
- 145 K. Sun, D. Tan, X. Fang, X. Xia, D. Lin, J. Song, Y. Lin, Z. Liu, M. Gu, Y. Yue and J. Qiu, *Science*, 1979, **2022**(375), 307–310.
- 146 X. Huang, Q. Guo, S. Kang, T. Ouyang, Q. Chen, X. Liu, Z. Xia, Z. Yang, Q. Zhang, J. Qiu and G. Dong, *ACS Nano*, 2020, **14**, 3150–3158.
- 147 H. Zhu, A. Liu, H. L. Luque, H. Sun, D. Ji and Y.-Y. Noh, *ACS Nano*, 2019, **13**, 3971–3981.
- 148 Y. Zhang, Y. Ren, X. Xie, Y. Wei, L. He, L. Fang, J. Zhang, Y. Yuan and P. Wang, *Adv. Funct. Mater.*, 2022, **32**, 2108855.
- 149 X. Zhu, R. Zhang, M. Li, X. Gao, C. Zheng, R. Chen, L. Xu and W. Lv, *J. Phys. Chem. Lett.*, 2022, **13**, 6101–6109.
- 150 D. Xu, Z. Gong, Y. Jiang, Y. Feng, Z. Wang, X. Gao, X. Lu, G. Zhou, J.-M. Liu and J. Gao, *Nat. Commun.*, 2022, **13**, 7020.
- 151 D. Yao, X. Mao, X. Wang, Y. Yang, N. D. Pham, A. Du, P. Chen, L. Wang, G. J. Wilson and H. Wang, *ACS Appl. Mater. Interfaces*, 2020, **12**, 6651–6661.
- 152 G. B. Adugna, S. Y. Abate, W.-T. Wu and Y.-T. Tao, *ACS Appl. Mater. Interfaces*, 2021, **13**, 25926–25936.
- 153 M. A. Triana, E.-L. Hsiang, C. Zhang, Y. Dong and S.-T. Wu, *ACS Energy Lett.*, 2022, **7**, 1001–1020.
- 154 A. S. de León, M. de la Mata, I. R. Sanchez-Alarcon, R. Abargues and S. I. Molina, *ACS Appl. Mater. Interfaces*, 2022, **14**, 20023–20031.
- 155 J. Wang, Y. Zhang, Y. Huang, G. Li, H. Chen, H. Li, Y. Liu and S. Chen, *Chem. Eng. J.*, 2022, **434**, 133866.
- 156 Q. Zhang, B. Wang, W. Zheng, L. Kong, Q. Wan, C. Zhang, Z. Li, X. Cao, M. Liu and L. Li, *Nat. Commun.*, 2020, **11**, 31.
- 157 M. N. An, S. Park, R. Brescia, M. Lutfullin, L. Sinatra, O. M. Bakr, L. de Trizio and L. Manna, *ACS Energy Lett.*, 2021, **6**, 900–907.